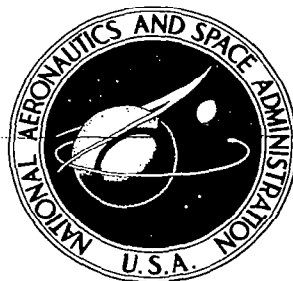


**NASA CONTRACTOR  
REPORT**



NASA CR-8

c.1

0060094



LOAN COPY  
KURT...

NASA CR-868

# PLASMA BOUNDARY INTERACTIONS

*by S. Aisenberg, P. Hu, V. Robotgi, and S. Ziering*

*Prepared by*  
SPACE SCIENCES, INC.

Waltham, Mass.

*for*

NATIONAL AERONAUTICS AND SPACE ADMINISTRATION • WASHINGTON, D. C. • AUGUST 1967



## PLASMA BOUNDARY INTERACTIONS

By S. Aisenberg, P. Hu, V. Rohatgi, and S. Ziering

Distribution of this report is provided in the interest of information exchange. Responsibility for the contents resides in the author or organization that prepared it.

Prepared under Contract No. NASw-1014 by  
SPACE SCIENCES, INC.  
Waltham, Mass.

for

NATIONAL AERONAUTICS AND SPACE ADMINISTRATION



## ABSTRACT

The interactions between moving plasmas and boundaries are studied theoretically and experimentally. The momentum and energy transport in the sheath is derived theoretically in terms of kinetic and moment equations. A new set of kinetic equations has been derived in order to allow for the microscopic incorporation of ionization phenomena. The tangential drag of the plasma on the cathode and the anode is studied experimentally and it is shown that the electrode drag is appreciable. The cathode drag is larger than the anode drag because of the positive ion current to the cathode. From the drag measurement it is possible to determine the ion current partitioning to the cathode. A theory of ion microfield emission is developed to explain the electron current emission from the cathode since the thermionic emission or field emission alone cannot account for the electron emission. The phenomena of arc retrograde motion is briefly studied and is explained in terms of a plasma phase propagation in the direction of increasing magnetic field where the ambipolar diffusion loss is reduced. The energy transport mechanisms to the electrode are analyzed to determine the dominant ones. An improved insulation structure for arc electrodes has been devised and used to increase electrode life. The problem of arc constriction is studied and it is shown that the constriction can be explained in terms of the balance between the input energy and the various energy loss modes. Experimental data is provided to confirm the theoretical dependence of arc diameter upon arc current, arc velocity, transverse magnetic field and upon reduced pressure.



# CONTENTS

<u>Section</u>		<u>Page</u>
	ABSTRACT	iii
1	INTRODUCTION	1
2	THEORY	7
	2.1 Plasma Sheath	8
	2.2 Kinetic Model of Ionization	12
	2.3 Electron Emission Mechanism	17
	2.4 Arc Constriction	27
	2.5 Analytical Study of Energy Transfer to Boundaries Using Continuum Theory	40
	2.6 Arc Retrograde Motion	50
3	EXPERIMENT	52
	3.1 The Electrode Drag Measurement	53
	3.1.1 Improved Insulators for Arc Electrodes	55
	3.1.2 Drag Measurement Instrumentation	58
	3.2 Analysis of Results of Drag Study	61
	3.3 Deduction of Current Partitioning at the Cathode	65
	3.4 Measurement of Arc Constriction and The Voltage Dependence of Cathode Fall in a Magnetic Field	71
4	SUMMARY	80
	ACKNOWLEDGMENT	82
	REFERENCES	83



## ILLUSTRATIONS

<u>Figure</u>		<u>Page</u>
1	Typical Ion Trajectories, $F_1^+ = F_6^+ \equiv 0$	10
2	Typical Electron Trajectories, $F_4^- \equiv 0$	11
3	Ion Current - Voltage Relation for the Case: $\alpha_1^+ = \beta_0^+ = \gamma^- = E_1 = 0$ , $\alpha_1^- + \beta_1^- = 1$ , $T^+ = T^- = T_0 = T$ , and $N^+ = N^- = N$ .	13
4	Emission Current Density and Vapor Pressure as a Function of Temperature	21
5	Electrons Emitted Per Incident Ion as Calculated by the Ion Microfield Emission Model (using average values)	26
6	Arc Diameter as a Function of Arc Current for an Atmospheric Pressure Nitrogen Arc (from data of Milliaris)	41
7	Energy Flux Transport to Anode by Various Plasma Components	44
8	Kinetic Energy as a Function of Specific Impulse - For Various Gases	46
9	Schematic of Rotary Electrode Structure for the Measurement of Tangential Electrode Forces	54
10	Metallic Insulators for Arc Electrodes	57
11	Circuit Diagram of RF Oscillator and Phase Sensitive Demodulator	59
12	Transient Response of Transducer System Which Measures the Tangential Electrode Force for an Arc in a Transverse Magnetic Field	60
13	Drag Force on Electrodes of a JxB Arc as a Function of Magnetic Field (at low pressure)	62
14	Electrode Drag Force vs. Magnetic Field in Helium	63

<u>Figure</u>		<u>Page</u>
15	Dependence of the Threshold B Field for Cathode Drag on the Arc Current	66
16	Dependence of Cathode Drag on Gas Pressure	67
17	Drawing of a Discharge Tube Showing the Electrode and Magnetic Field Configuration	72
18	Dependence of Cathode Spot Width Upon Arc Current for Constant Magnetic Field and Pressure	74
19	Dependence of Arc Width Upon Magnetic Field for Constant Pressure and Arc Current	76
20	Variation of Arc Width as a Function of Mercury Vapor Pressure (for constant magnetic field and arc current)	77
21	Dependence of Arc Voltage Upon Transverse Magnetic Field and Upon Mercury Vapor Pressure	78

## 1. INTRODUCTION

The past two decades have seen the rapid growth of a new discipline in physics concerned with the "fourth state of matter" namely, plasma physics. This recent activity has been motivated by the natural occurrence of plasmas in the space environment, and by the search for the practical utilization and application of new devices (such as plasma generators and accelerators) based on these concepts. There is, however, one critical area which needs to be fully understood before engineering applications associated with this "fourth state of matter" can be exploited on a large scale. This is the interaction of a plasma with the physical boundaries, by means of the intermediate plasma boundary layers. It is quite evident that designers of useful and practical devices utilizing plasmas in some form or other, have to face realistically the problem of physically constraining the hot plasma and, therefore, must obtain an understanding of the physical processes governing plasma-boundary interactions. Also, the interaction between a space vehicle and its environment additionally focuses on the need of a better understanding of plasma-boundary layers.

From a practical point of view, a more detailed understanding of the interaction between high energy plasmas and plasma boundaries remains an important problem associated for instance with JxB accelerators and MHD generators. This is the case because the efficiency and life of plasma accelerators are limited by the excessive power dissipation at the electrodes. In addition, the momentum transferred to the electrodes reduces the effectiveness of the accelerator. An understanding of the basic processes involved in plasma-boundary interactions is therefore necessary in order to aid in the systematic improvement of high power plasma machines.

The research program conducted at Space Sciences, Inc. over a two year period under NASA sponsorship thus concerned itself with an investigation of the basic physical processes governing the interaction of plasma and electrodes, as

well as with the more general problem of plasma-boundary interactions. This study was conducted on both a theoretical and an experimental level. The central theme of the study was the various physical aspects of plasma-boundary layers resulting from direct contact of a plasma with surfaces. In addition to the specific motivation for this study provided by the current accelerator research, the field of plasma-surface interactions has many diverse and practical applications and is of fundamental interest in the expanding technology concerned with plasma research.

The basic plasma boundary layer problem arises from the requirement of physically preventing a hot plasma ( $10,000^{\circ}\text{K}$  and above) from catastrophically destroying the machine environment, while the plasma performs its essential mission which is most often some form of energy exchange. While the body of the plasma is relatively isotropic, it is clear that any constraining physical boundaries will introduce large thermal and viscous gradients. Thus a clearer understanding of the nature of these gradients and the basic physical mechanisms controlling them is absolutely essential. This is especially true because of the limited range of materials able to withstand even moderate temperatures (when compared to  $10,000^{\circ}\text{K}$ ), especially since we may also require these materials to have desirable electrical properties when they function as electrodes. Our understanding is furthermore complicated in that the boundary layer is a transition zone in which continuum concepts (magnetohydrodynamic theories) do not apply. Because of the effects introduced by the physical boundaries, the particle distribution functions are far from isotropic and even become discontinuous at the boundary itself. In these domains (boundary layer) new theoretical concepts have to be developed to treat the expected physical situation. At the same time diagnostic measurements in the boundary layer (also referred to as the plasma sheath) are exceedingly difficult.

There are six separate sections which summarize the theoretical effort at Space Sciences during the course of the program (Section 2.1 through 2.6). The first concerns itself with the basic structure of a plasma sheath as a result

of a planar electrode interacting with a steady state plasma. Care has been taken to incorporate the most general boundary conditions and not to assume "a priori" the usual assumption of monoenergetic incident ions or complete absorption at the electrode surface. The successful completion of this phase of the work in a general form, as summarized below in Section 2.1 and detailed in Ref. 1, now allows us to extend these results to more practical problems. An immediate extension is the consideration of the actual flow conditions encountered for instance in JxB accelerators or in MHD generators. Here we deal with a plasma moving in a direction parallel to the surface (electrode). Thus under the continuation of this program the fundamental sheath in the presence of transverse flows is being examined, and considerable progress has been made at this time<sup>2</sup>. This extension will also allow us under the continued program to correlate the experimental program with the theoretical effort. Thus the incorporation of transverse flows in the theory will allow for a direct comparison with the experimental work on drag at the electrode carried out in this program.

A further idealization usually made in sheath investigations concerns the neglect of ionization effects. It was found necessary to develop kinetic model equations which retain the effects of ionization in a microscopic analysis in order to subsequently utilize these equations for a more precise analysis of sheath phenomena. These equations were successfully constructed<sup>3</sup>, as summarized in Section 2.2 below.

Of considerable importance to the study of boundary layer interactions is the current partitioning between ion impingement and electron emission at the cathode spot. In general, the presence of tangential electrode frictional forces is expected for a hot plasma flowing in a channel when one considers that some of the tangential momentum is transferred each time an electron, ion, or gas atom collides with the surface. In particular, it has been suggested by Thom, Norwood and Jalufka<sup>4</sup>, that there are appreciable drag forces on the plasma near the cathode because of the momentum exchange between the positive ions and the cathode. Thus the ion current partitioning at the cathode spot is expected to influence the cathode drag forces.

In order to demonstrate the importance of this effect, the ion current drag and ion current partitioning was examined both theoretically and experimentally in this program. The process of electron emission was analyzed and it was shown that the ion current to the cathode is an essential feature of the electron emission process. A theory of ion induced electron emission (microfield emission) is presented in Section 2.3. Direct experimental measurements of the tangential electrode drag for a cathode and for an anode in a  $J \times B$  accelerator (as described in Section 3.1) showed that there is indeed a significant ion current contribution to the cathode drag. The results of the ion current drag measurements have been used to deduce the ion current partitioning at the cathode spot and are discussed in Sections 3.2 and 3.3. As part of the problem of electrode drag at the cathode the phenomena of retrograde motion was studied and it was concluded that retrograde motion corresponds to plasma phase velocity and not retrograde particle velocity. Thus the retrograde motion is not expected to influence the drag measurements on the electrodes. The theory of arc retrograde motion as developed during this program is outlined in Section 2.6.

The severity of the electrode interaction and damage is related to the constricted nature of the discharge which is responsible for very high local power densities. For this reason, the theory of the arc constriction mechanism has been developed and a brief treatment is given in Section 2.4, while in Section 3.4 comparison is made with experimental data.

In order to assess the relative importance of various contributions to the energy transport to the boundaries, a comparison was made of the various related physical processes, and a brief description is presented in Section 2.5.

In the process of running the research arcs for data taking, it was found necessary to extend the electrode lifetime by devising composite metallic and dielectric insulators. The design of improved insulators has been published<sup>5</sup> and is discussed in Section 3.4.

Because of the importance of the cathode sheath drop, the effect of a transverse B field on the cathode fall was also studied and is briefly described in Section 3.6.

A number of the specific research conclusions as a result of this program have been published in the professional literature. Some of these are preliminary in the sense that in the development of new theories certain specific considerations had to be sacrificed in order to provide solutions of general scientific interest. On the other hand these solutions can be extended to more general as well as specific problems, and will illuminate some specific area of concern for plasma machines. A continuation of the research project described here is currently in progress. Thus for instance, the theoretical work developed here for the collisionless plasma sheath has been extended to include transverse flows. This extended effort makes direct contact with the physical situation encountered by plasma machines.

In the following report we shall summarize and bring together the various results obtained at Space Sciences in the performance of this contract. No attempt will be made to duplicate all the details of the various technical publications that have been made. Rather, it is anticipated that sufficient detail will be given, to allow the interested reader to decide whether or not the detailed references will be of interest. In certain instances where under the existing continuing program new preliminary results have been generated, they will be discussed. Section 2 will primarily be devoted to theory, while Section 3 will review the experimental part of the program. A summary of the program will be presented in Section 4.

The following reports and publications have resulted from this program and should be consulted for additional details:

## REPORTS, PUBLICATIONS, AND PRESENTATIONS

- S. Aisenberg, P. Hu, V. Rohatgi, and S. Ziering, "A Study of Electrode Effects in Crossed Field Accelerators," Summary Report, Contract NASw-1014, prepared for National Aeronautics and Space Administration (1965).
- P. N. Hu and S. Ziering, "Kinetic Model for Three Component Plasmas with Ionization," *Physics of Fluids*, 9, 1983 (1966).
- P. N. Hu and S. Ziering, "Collisionless Theory of a Plasma Sheath Near an Electrode," *Physics of Fluids*, 9, 2168 (1966).
- S. Aisenberg and V. Rohatgi, "A Study of Arc Constriction Processes," presented at the Seventh Symposium on the Engineering Aspects of Magnetohydrodynamics, March 1966.
- S. Aisenberg and V. Rohatgi, "Measured Tangential Electrode Forces for an Arc in a Transverse Magnetic Field," *Applied Physics Letters*, 8, 194 (1966).
- V. Rohatgi and S. Aisenberg, "Composite Metallic and Dielectric Insulators for High Current Arc Electrodes," *Rev. Sci. Instr.*, 37, 1603 (1966).

## 2. THEORY

In most plasma devices it is found that the fully developed physical parameters in the interior of the plasma, while not completely understood by any means, can be analyzed with a fair expectation of realistically describing the physical situation by continuum theory. The main uncertainty however is in the transition domain between the bulk of the plasma and the physical boundary surface; that is in the sheath itself. In this latter domain of the plasma sheath, large deviations from equilibrium conditions are observed and a microscopic kinetic theory treatment is essential. (For a more detailed discussion of the respective domains and regions of validity as developed in this program, see Refs. 1 and 3.) Thus an analysis of the plasma sheath by kinetic theory techniques has received the major attention in the theoretical portion of the program.

Sections 2.1, 2.2 and 2.3 are concerned with the microscopic structure and boundary conditions for the plasma sheath. The extremely large variations of the physical parameters across the plasma sheath, between the fully developed plasma and the physical boundary (electrode), dictate the use of discontinuous distribution functions. Thus Section 2.1 (and the more detailed discussion in Ref. 1) critically examines the conventional theories and establishes a new theory for the plasma sheath. In order to fully consider the effects of ionization in the sheath, it was found necessary to incorporate the phenomena of ionization in a set of kinetic equations as no such formalism was available. Section 2.1 (as well as the more detailed discussion in Ref. 3) discusses a new set of kinetic equations which allow for the introduction of ionization as a microscopic phenomena into the theory, rather than the usual 'ad hoc' introduction of ionization as a gross parameter. From a microscopic point of view it is important to determine the mechanism of electron emission from the cathode in order to prescribe the proper boundary conditions for the plasma sheath at the cathode. Thus a possible mechanism for the electron emission process is discussed in Section 2.3 below.

While continuum theory is inadequate for a detailed analysis of the sheath, it is possible to obtain some gross parameters and order of magnitude estimates. Section 2.4 below summarizes the work on the arc constriction process, and offers a possible explanation for this important observed effect. An analytical study of energy transfer to boundaries by continuum theories is presented in Section 2.5. The final Section 2.6 discusses a theory for the phenomena of retrograde arc motion.

## 2.1 Plasma Sheath

Near an electrode, because of the interaction between the plasma and the physical boundary, there is a layer, called a "sheath", where the plasma is no longer neutral and a strong electric field can exist. Since the Debye length is a measure of the distance over which the electron density can deviate from the ion density in the absence of a magnetic field (see, e.g. p. 17 in Ref. 6), it is clear that the thickness of a plasma sheath is of the order of the Debye length. Thus, if the mean free path of the plasma is larger than the Debye length, most of the collisions between particles will occur outside the sheath and the plasma in the sheath can be considered as collisionless.

There are various sheath models based on the assumption that the plasma in the sheath is collisionless. Restrictions as well as ranges of validity for various existing sheath models have been discussed in detail in Ref. 1. The most widely applied sheath model is based on the following assumptions:

- (1) Attracted particles are monoenergetic and are completely annihilated at the surface of electrode.
- (2) Repelled particles are in a Maxwellian distribution and are completely and specularly reflected at the electrode.

As a result of the above assumptions, this sheath model is subject to the following restrictions:

- (1) A stable sheath structure can only be established when the so-called "Bohm's sheath criterion" is satisfied. The

criterion states, in the usual form, that the attracted particles at the sheath edge must stream towards the electrode at a velocity greater than the thermal speed of the repelled particles.

- (2) The electric current contributed by the attracted particles in a one dimensional case is always constant, regardless of either the electrode temperature or the voltage drop across the sheath.

In order to develop a self-consistent sheath model that is free from the above restrictions, we have, in Ref. 1, examined the collisionless theory in very general terms and have found that the main difficulty arises from the assumption of complete annihilation of the attracted particles. Physically, it is true that an electrode at low temperature will neutralize most of the attracted particles, however, the mere presence of the diffuse reflection mechanism will allow the accumulation of the number of attracted particles trapped near the electrode until a stable structure of the sheath is established.

Consequently, we have developed a new sheath model by incorporating very general boundary conditions at the electrode as well as at the sheath edge. Specifically, we allow the attracted particles to be in a Maxwellian distribution at the sheath edge and to be reflected, both specularly and diffusely, from the electrode. Furthermore, the electrode may emit particles.

Since the total energy (kinetic and potential) of a particle does not change in the sheath in the absence of collisions, particles can be identified by their energies. Depending on the energy a particle carries at the respective boundary (the electrode or the sheath edge), particles can be divided into several groups. Typical trajectories of electrons and ions of various groups near a cathode are illustrated in Figures 1 and 2.

In the new model, a monotonic sheath structure can be obtained without the usual criterion. Explicit results for the current-voltage relation as well as for the sheath thickness are derived in detail in Ref. 1. Other important physical quantities are expressed in terms of the electrostatic potential which can be

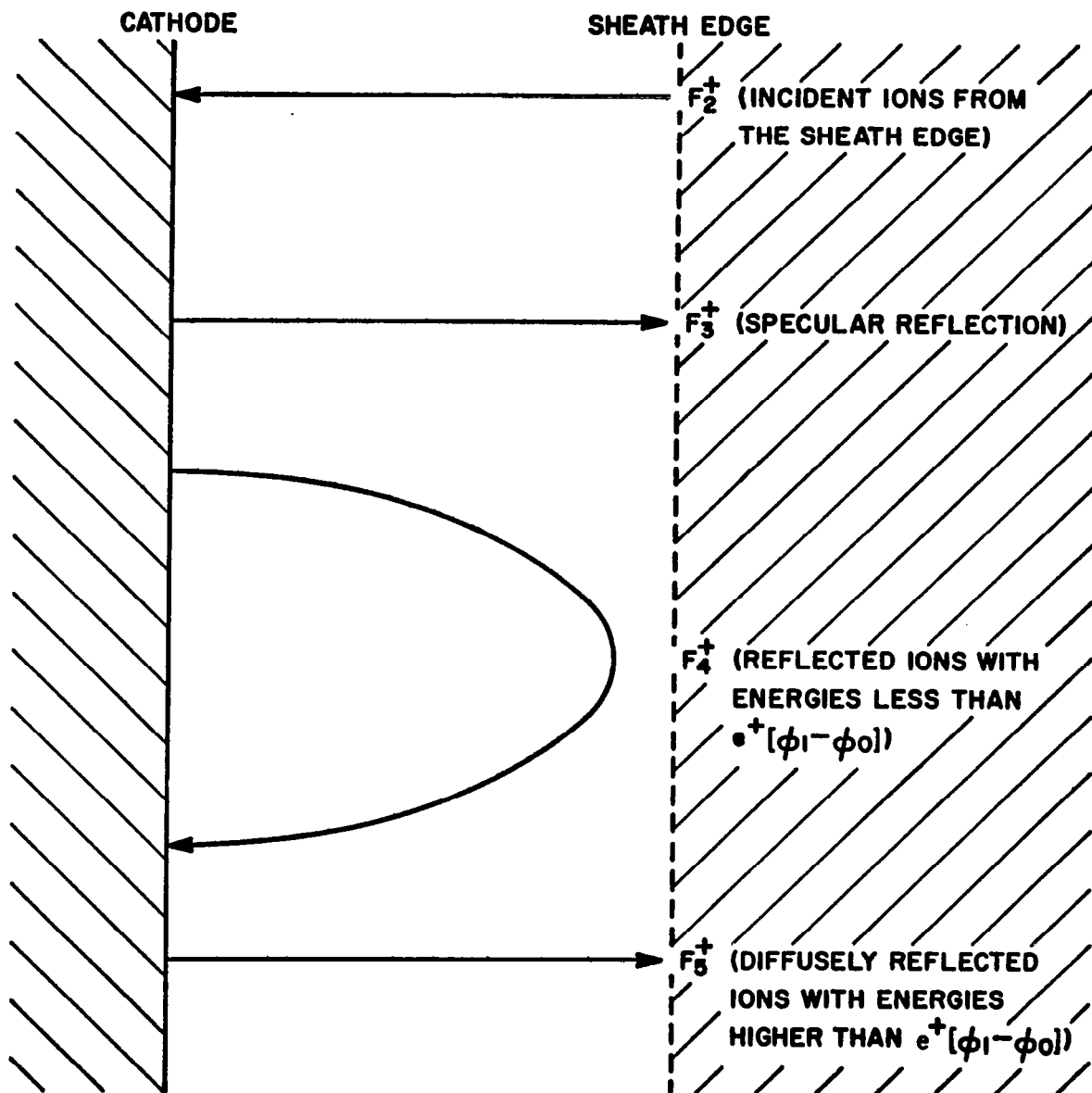


FIGURE 1.  
 TYPICAL ION TRAJECTORIES  
 $F_1^+ = F_6^+ = 0$

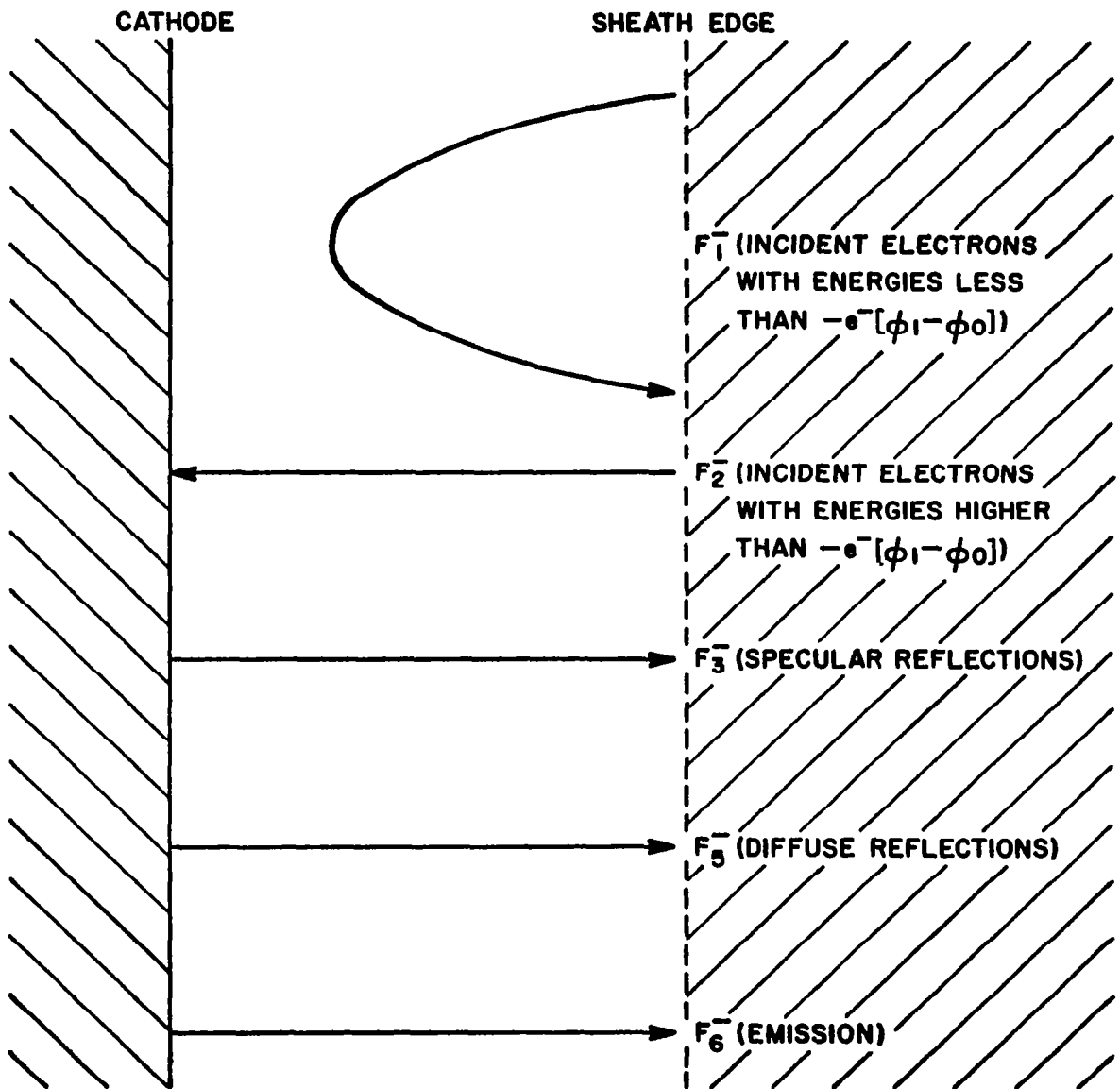


FIGURE 2.  
 TYPICAL ELECTRON TRAJECTORIES  
 $F_4^- = 0$

calculated by a quadrature subject to the physical parameters to be specified. The general solution reduces to a simple analytic form for the special case where the temperatures of the electrons, the ions and the electrode are identical. The ion-current-voltage relation for the special case is plotted in Figure 3. It is seen that the ion current increases monotonically with the potential difference across the sheath and reaches the saturation ion current asymptotically.

## 2.2 Kinetic Model of Ionization

For the problem of a cathode sheath, a part of the incident ions are assumed to be annihilated by the electrode. The reflected and neutralized particles, leaving the electrode, are eventually ionized again through collisions with other particles. As mentioned in the preceding section, the thickness of a plasma sheath is of the order of the Debye length in the absence of magnetic field. Thus, most of the ionization will take place outside the sheath if the mean free path for the ionizing collisions is larger than the Debye length. The condition at the sheath edge, although it is usually taken as the boundary condition for the collisionless sheath, should actually be determined through the incorporation of the ionization process.

On the other hand, if the mean free path is much smaller than the Debye length, the ionization process will occur between the electrode and the sheath edge and will therefore determine the boundary condition for the sheath in the continuum domain.

For the general case where the mean free path is neither large nor small as compared with the Debye length, the ionization is taking place in the sheath and the problem cannot be treated without a kinetic description of the ionization process.

In Ref. 3 we have developed a kinetic model for a three-component plasma with ionization based on the following assumptions:

- (1) Ionization is solely caused by electron-neutral collisions.

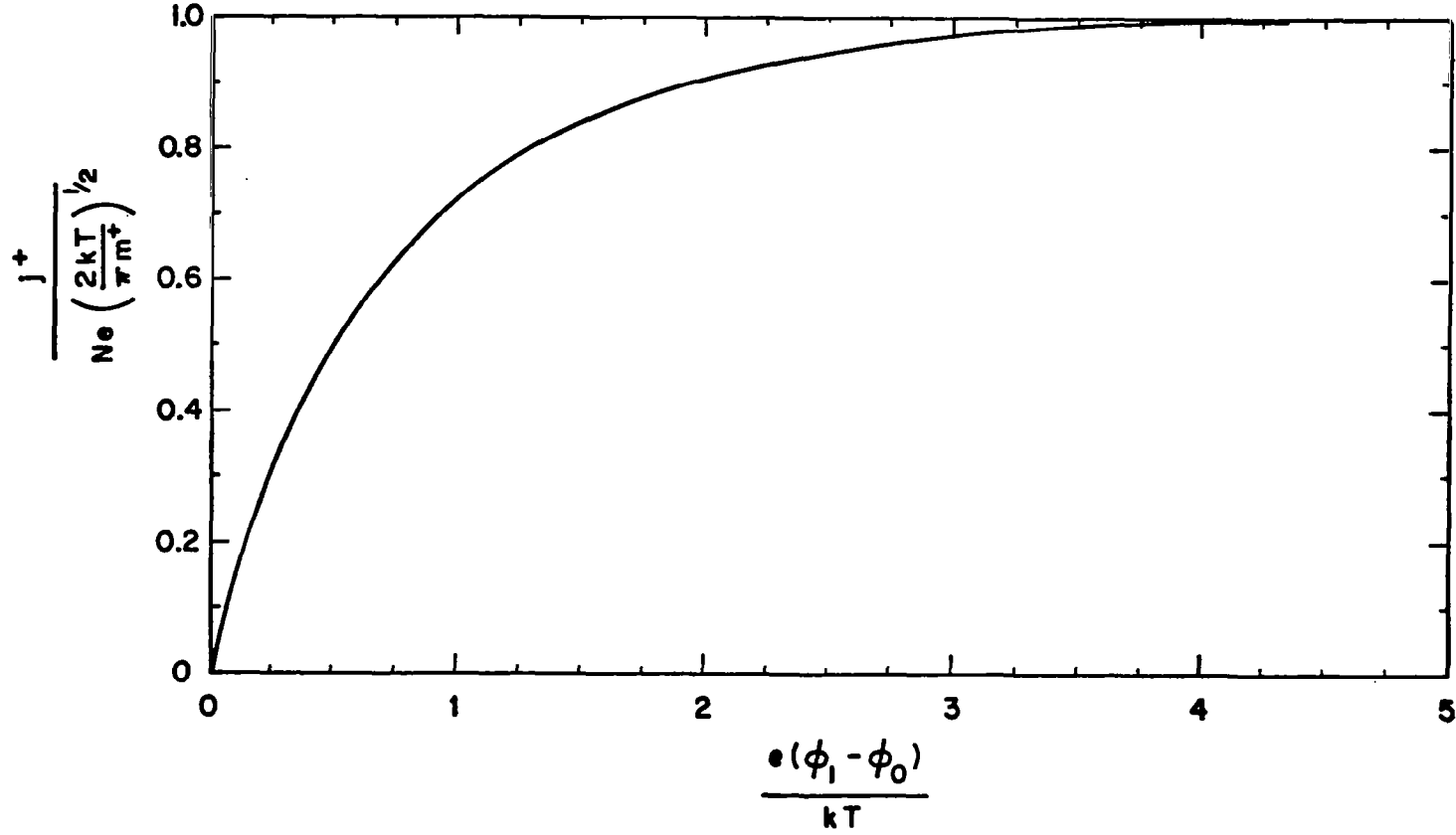


FIGURE 3.

ION CURRENT - VOLTAGE RELATION FOR THE CASE:  $\alpha_1^+ = \beta_0^+ = \gamma^- = E_1 = 0$ ,  
 $\alpha^- + \beta^- = \beta_1^+ = 1$ ,  $T^+ = T^- = T_0 = T$ , and  $N^+ = N^- = N$ .

- (2) All other collisions are elastic.
- (3) During an electron-neutral collision, the electron that has a kinetic energy higher than the ionization potential of the neutral particles will ionize the neutral with a certain probability.
- (4) During the ionizing collision, both the ionization and the relaxation processes are taking place simultaneously.

Denoting the electron, the ion and the neutral, respectively by the subscripts 1, 2, and 3, the mathematical system can be written as:

$$D_1 f_1 = \sum_i \frac{n_i}{\sigma_{1i}} (f_{1i} - f_1) + \frac{\alpha n_1}{\sigma_{13}} f_{31} + \frac{\alpha n_3}{\sigma_{13}} \left[ f'_{13} - f_{13} H(v-v_0) \right] \quad (1)$$

$$D_2 f_2 = \sum_i \frac{n_i}{\sigma_{2i}} (f_{2i} - f_2) + \frac{\alpha n_1}{\sigma_{13}} f_{31} \quad (2)$$

$$D_3 f_3 = \sum_i \frac{n_i}{\sigma_{3i}} (f_{3i} - f_3) - \frac{\alpha n_1}{\sigma_{13}} f_{31} \quad (i = 1, 2, 3) \quad (3)$$

the right-hand sides represent the rate of change of the distribution functions and the left-hand sides represent the usual differential operations which can be written as:

$$D_i f_i = \frac{\partial f_i}{\partial t} + \underline{v} \cdot \frac{\partial f_i}{\partial \underline{x}} + \underline{a}_i \cdot \frac{\partial f_i}{\partial \underline{v}} \quad (4)$$

where  $\underline{x}$  and  $\underline{v}$  are respectively the position and velocity vectors of the particle and  $\underline{a}_i(\underline{x}, \underline{v}, t)$  is the acceleration of a particle of species  $i$  due to body forces.

In Eqs. (1) through (3),  $f_{ij}$  is a local Maxwellian distribution defined as;

$$f_{ij} = n_i \left( \frac{m_i}{2\pi k T_{ij}} \right)^{3/2} \exp \left[ - \frac{m_i (\underline{v} - \underline{u}_{ij})^2}{2k T_{ij}} \right] \quad (5)$$

where  $n_i$ ,  $\underline{u}_{ij}$  and  $T_{ij}$  are, respectively, the density, the velocity, and the temperature given by;

$$n_i = \int f_i \, d\underline{v} \quad (6)$$

$$n_i \underline{u}_{ii} = n_i \underline{u}_i = \int \underline{v} f_i \, d\underline{v} \quad (7)$$

$$3 n_i k T_{ii} = 3 n_i k T_i = m_i \int (\underline{v} - \underline{u}_i)^2 f_i \, d\underline{v} \quad (8)$$

$$(m_i + m_j) \underline{u}_{ij} = m_i \underline{u}_i + m_j \underline{u}_j \quad (9)$$

$$T_{ij} = T_i + \frac{2m_i m_j}{(m_i + m_j)^2} \left[ (T_j - T_i) + \frac{m_j}{6k} (\underline{u}_j - \underline{u}_i)^2 \right] \quad (10)$$

with  $m_i$  as the mass of the particle and  $k$  as the Boltzmann constant. The integrals in Eqs. (6) through (8) are to be carried out in the complete velocity space.

In Eq. (1)  $f'_{13}$  represents the local Maxwellian distribution of an electron after it ionized a neutral particle and is given by;

$$f'_{13} = n'_1 \left( \frac{m_1}{2\pi kT'_{13}} \right)^{3/2} \exp \left[ - \frac{m_1 (\underline{v} - \underline{u}_{13})^2}{2kT'_{13}} \right] \quad (11)$$

$$n'_1 = n_1 \left[ \operatorname{erf} c \left( \frac{m_1 v_o^2}{2kT'_{13}} \right)^{1/2} + \left( \frac{2m_1 v_o^2}{\pi kT'_{13}} \right)^{1/2} \exp \left( - \frac{m_1 v_o^2}{2kT'_{13}} \right) \right] \quad (12)$$

and,

$$3n'_1 kT'_{13} = 3n_1 kT_{13} - n_1 m_1 v_o^2 \operatorname{erf} c \left( \frac{m_1 v_o^2}{2kT'_{13}} \right)^{1/2} \quad (13)$$

with the complementary error function defined by;

$$\operatorname{erf} c x = 2\pi^{-1/2} \int_x^\infty \exp(-t^2) dt$$

and  $v_o$  as the electron speed that is equivalent to the ionization potential of the neutral particle. Thus  $n'_1$  is the density of electrons which have kinetic energies higher than the ionization potential. Since the possibility of ionization depends on many factors, we have introduced  $\alpha$  as the probability of ionization which has to be determined by other means. Therefore, in Eqs. (1) through (3)  $\alpha n'_1 / \sigma_{13}$  is actually the ionization frequency and the last term in Eq. (3) represents the neutral particles lost in ionization while the corresponding terms in Eqs. (1) and (2) represent the creation of electrons and ions. With the step

function  $H(v - v_0)$ , the quantity in the brackets of Eq. (1) represents the change of the electron distribution function during the ionization process.

Details of the derivation of the above equations can be found in Ref. 3.

### 2.3 Electron Emission Mechanism

The purpose of this section is to show the importance of the positive ions in producing the electron emission at the cathode. The ion current partitioning at the cathode is a vital factor in setting the plasma sheath boundary conditions and is also a determining factor in the additional cathode drag due to ions in  $J \times B$  accelerators and in MHD generators. An analysis was therefore made of the various possible electron emission mechanisms and it was shown for non-refractory electrodes (and possibly for refractory electrodes) that the electron emission is probably not due to thermionic emission or to field emission. (The possibility of combined thermionic and field emission was briefly considered but has not yet been analyzed in complete detail.)

One important conclusion of this section is that for the most probable methods of electron emission from the arc cathode that can be postulated, it is necessary to consider the positive ion current to the cathode as an essential feature required to account for the emission. Even though the ion current to the cathode may be a small fraction of the total cathode current, this ion current is needed to supply the thermionic heating power or else to supply the strong electric field necessary for field emission. Standard field emission processes are not capable of explaining the low current densities. To be proposed in this section is a method of accounting for the electron emission by a modified field emission process due to the micro electrostatic fields of the positive ions flowing to the cathode. A similar mechanism has been considered by Kisliuk<sup>7</sup> in connection with voltage breakdown. All of these methods of explaining the electron emission for an arc "cold" cathode (not heated externally) require the flow of positive ions to the cathode spot as an essential feature of the emission processes.

An analysis has been made of the possible electron emission processes for tungsten cathodes. While the thermionic emission may be an acceptable process for thoriated tungsten it does appear to be questionable for non-thoriated tungsten and particularly for lower melting point cathodes such as copper. Another problem is that the work function of a thoriated tungsten cathode is low only when the cathode is at temperatures of about 1950 to 2,000°K. At other temperatures the balance between the out diffusion and evaporation of thorium may not be satisfied and a surface coverage of thorium may not be maintained.

In any event, if thermionic emission is assumed to be the dominant mechanism it is necessary to account for the power required to maintain the high cathode temperature. For a low pressure plasma where radiation heating of the cathode is low, a significant part of the heating power must be supplied by the positive ion current, so that the ion current to the cathode is an important part of the thermionic emission process.

The requirement for high cathode temperature can be relaxed if methods can be postulated that could result in the significant reduction of work function. Two possible methods have been studied but it appears that they are not large enough to appreciably reduce the work function. The first is the possible reduction of work function as the cathode spot goes into the liquid phase. The density change associated with the change of phase is about 20% or less. The interatomic distance therefore is increased by about 7%. If we assume that the work function is predominately due to the mirror image forces at the metallic surface, then the work function should be inversely proportional to the interatomic spacing. Thus one expects that the work function of the liquid phase should be only about 7% less than for that of the solid metal. This will result in a possible reduction of thermionic emission temperature of only about 7%, and is not large enough to be significant.

A second way of reducing the work function is through the Schottky effect where a strong external field can reduce the work function for thermionic emission<sup>8</sup>. If this effect were to be significant, then positive ion current to the cathode would

be necessary to supply the strong electron field required. It can be shown, however, that if the electron field were large enough to give an appreciable reduction of work function, the field emission would be orders of magnitude larger. Only if the cathode temperature is large can the Schottky enhanced emission be large compared to the field emission.

It is possible to explain very high current densities by field emission where the strong field required at the surface is produced by the positive ion current flowing to the cathode. There is a relation between the cathode field strength and the positive ion current which can be calculated from MacKeown's equation<sup>9</sup> for the bipolar space charge sheath. At the same time, the field emission current (for a given work function) can be calculated in terms of this electric field. It appears however, that field emission can be used as an explanation of the observed electron emission only for current densities above  $10^7$  amp/cm<sup>2</sup> and even then for very favorable work functions where  $\phi = 2V^{10}$ . The observation of low current densities ( $J = 5 \times 10^3$  amp/cm<sup>2</sup>) can be explained by pure field emission only if mechanisms are postulated to reduce the work function.

The required cathode spot temperature will be calculated here for the case of assumed thermionic emission current from a thoriated tungsten cathode. If the arc current is 50 amps and the cathode spot diameter is about 1mm then the current density is about  $5 \times 10^3$  amp/cm<sup>2</sup>. This value appears to be explainable in terms of thermionic emission only if a high temperature spot can be assumed. The actual cathode spot size is hard to determine but can be estimated from damage tracks observed for JxB accelerators. For an arc of about 10 amps in argon the measured spot size on a molybdenum cathode is about 0.18 mm in diameter corresponding to a current density of about  $4 \times 10^4$  amp/cm<sup>2</sup>. There is also the question of what fraction of the observed cathode current can be ascribed to thermionic emission and what fraction is due to ion collection. Measurement obtained on this research program can be interpreted as showing that about 10% of the cathode is due to positive ion current.

The thermionic emission current density  $J$ , can be calculated from the Richardson-Dushman equation,

$$J \text{ (amp/cm}^2\text{)} = A_R T^2 \exp(-\phi_R/V_T) \quad (14)$$

where  $A_R$  and  $\phi_R$  (volts) are the Richardson constants,  $T$  is the temperature in  $^\circ\text{K}$ , and  $V_T = T/11,605$ . The thermionic emission calculated for thoriated-tungsten for  $A_R = 4 \text{ amp/cm}^2/\text{K}^2$  and  $\phi_R = 2.85 \text{ volt}$ <sup>11</sup> is shown in Figure 4 along with the vapor pressure of tungsten<sup>12</sup> as a function of temperature. It can be seen that an emission current density of  $5 \times 10^3 \text{ amp/cm}^2$  can be obtained for a temperature of about  $3600^\circ\text{K}$ . The corresponding vapor pressure of  $W$  at this temperature is about  $2 \times 10^{-2} \text{ Torr}$ . This neglects the effect of the thorium on the vapor pressure of tungsten. Actually the vapor pressure of thorium is about an order of magnitude greater than tungsten at the same temperature so that the thorium coverage is expected to decrease unless the out diffusion rate of thorium from the bulk is faster than the evaporation rate.

It is possible that pure thermionic emission is not the dominant process at the cathode spot for  $W\text{-Th}$ , and certainly not the process for lower melting point cathodes such as mercury and copper.

A simple calculation has been made of the maximum cathode spot temperature for typical conditions using simplified conditions, and it has been shown that the maximum cathode spot temperatures will be small relative to those required for thermionic emission.

If one assumes that the cathode spot is cooled only by thermal conductivity and that the heat flow pattern can be approximated by a hemispherical geometry, then the steady state spot temperature can be computed in terms of the spot input power, the spot diameter, and the thermal conductivity of the cathode. For a representative case of 50 watts input power, and a current density of  $10^5 \text{ amp/cm}^2$

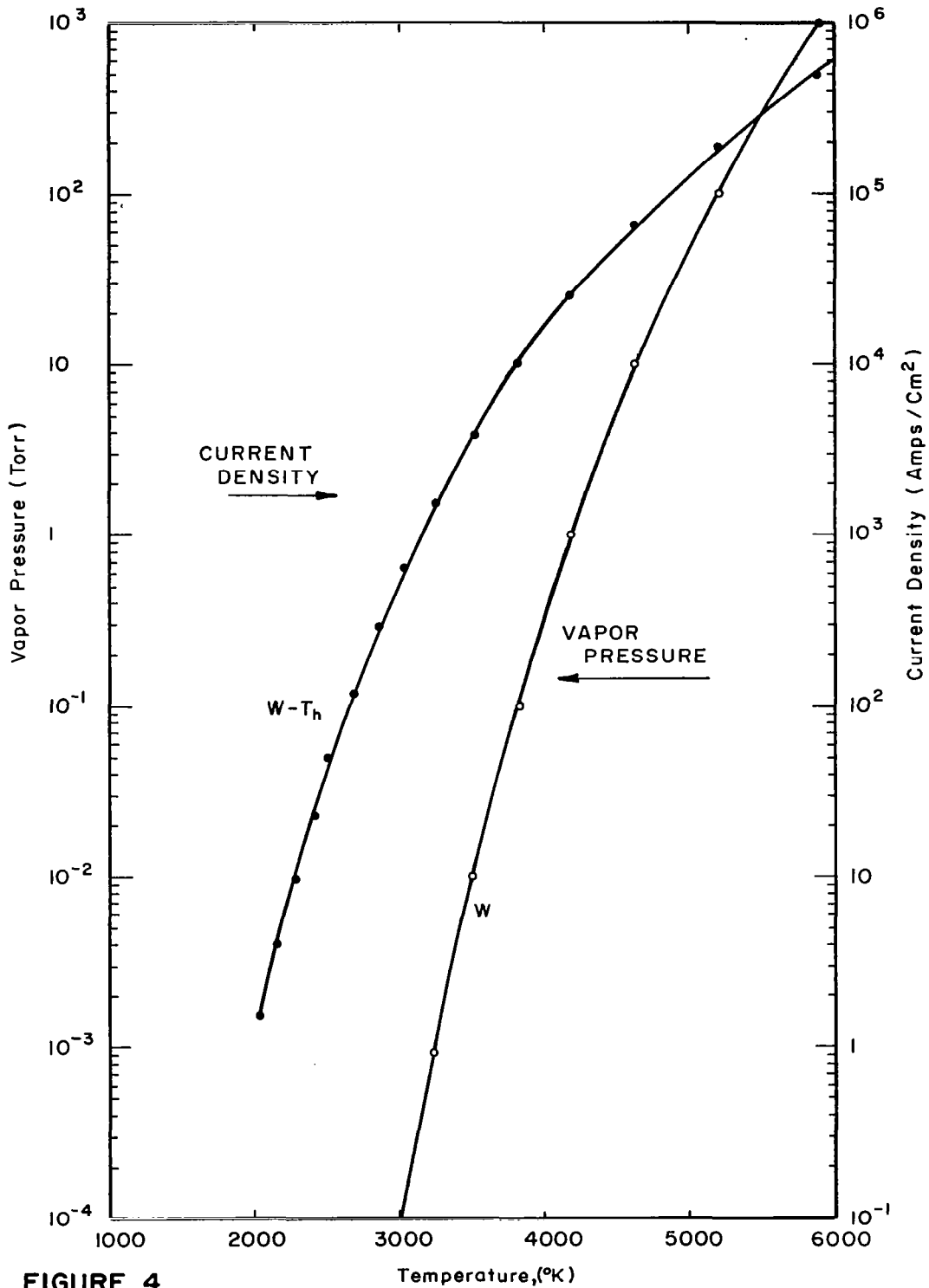


**FIGURE 4.**  
**EMISSION CURRENT DENSITY AND VAPOR PRESSURE**  
**AS A FUNCTION OF TEMPERATURE.**

or less, the computed spot temperature for electrodes such as Cu, Mo, W is less than 2000°K and is not enough for thermionic emission.

To be proposed is a micro-field emission model that can result in a significant number of electrons emitted per incident positive ion. The calculations are still in the preliminary stage, but order of magnitude calculations will be presented to illustrate the physical processes involved and to demonstrate the feasibility of the mechanism.

The usual model of field emission caused by the positive ion current to the cathode calculates the space charge field in terms of the average ion charge density and does not take into account the local electric field that is associated with each individual ion. The local electric field can be much larger than the average electric fields. Since the field emission process is a strongly non-linear one, the field emission calculated from the local fields can be much larger than that for the average electric fields. It is this enhanced electric field associated with each ion that can result in appreciably enhanced electron emission. A similar model based upon the statistical fluctuations of space charge has been presented by Ecker and Müller<sup>8,13</sup>.

The electric field at a distance  $s$  from a positive ion with a charge  $q$  is,

$$E = \frac{q}{4\pi\epsilon_0 s^2} \text{ (MKS)} \quad (15)$$

where,

$$\begin{aligned} \epsilon_0 &= 8.85 \times 10^{-12} \text{ farad/meter} \\ s &= \text{meters} \\ q &= 1.602 \times 10^{-19} \text{ coulomb.} \end{aligned}$$

Because of the mirror image charge developed in a conducting surface near the ion, the field is increased by a factor of 2 (from symmetry). If the distance from the ion to the surface is  $s$  the electric field  $E_n$  normal to the surface and at

the intersection with the surface of the normal projection passing through the charge is,

$$E_n = \frac{2q}{4\pi\epsilon_o s^2} \quad (16)$$

As the ion comes very close to the cathode, the electric field can become very large. A few examples are presented in Table 1 where the perpendicular electric field  $E_n$  in volts per cm is given for various distances.

The distribution of the normal field along the surface can be specified to help evaluate the approximate emitting area. The normal electric field  $E_n$  is a function of distance  $D$  from the root of the normal projection and is given by

$$E_n = \frac{s}{(s^2 + D^2)^{1/2}} \cdot \frac{2q}{4\pi\epsilon_o (s^2 + D^2)} \quad (17)$$

From the data for the field emission current as a function of electric field as given by Good and Muller<sup>14</sup> it can be seen that the current density decreases by about a factor of 2 when the  $E$  field is decreased by about 10% (at about  $J = 10^5$  to  $10^6$  amp/cm<sup>2</sup>). In this range the distance  $D$  corresponding to a reduction of  $E_n$  by a factor of 10% is given by  $D = 1.9 s$  so that the dimensions of the field emitting spot is comparable to the distance of the ion from the surface.

Table 1 gives values of the average emitting area as computed by assuming that the radius of the emitting area is equal to the distance  $s$ . A more detailed calculation of this factor is recommended.

The question now is how much current can be emitted from this small area in the transit time of the ion to the surface. The transit time to the surface from a distance  $s$  can be calculated assuming a constant velocity  $v$  corresponding to the energy  $qV_s$  gained in going through the sheath potential drop  $V_s$ . The

TABLE 1

ELECTRONS EMITTED PER INCIDENT ION AS A RESULT OF THE INDIVIDUAL-ION-FIELD EMISSION MECHANISM

<u>Distance to Surface</u> <u>s(10<sup>-8</sup> cm)</u>	<u>Mirror Image Field</u> <u>E<sub>n</sub> (V/cm)</u>	<u>Field Emission Current Density</u> (a) <u>J<sub>F</sub> (A/cm<sup>2</sup>)</u>	<u>Average Emitting Area</u> <u>(10<sup>-15</sup> cm<sup>2</sup>)</u>	<u>Ion Transit Time</u> (b) <u>(10<sup>-14</sup> sec)</u>	<u>Average Field Emitted</u> <u>Electrons/ion</u> (a),(b)
2	7.20 x 10 <sup>8</sup>	3.4 x 10 <sup>11</sup>	1.3	2.88	77
3	3.20 x 10 <sup>8</sup>	9.8 x 10 <sup>10</sup>	2.8	4.32	75
4	1.80 x 10 <sup>8</sup>	1.7 x 10 <sup>10</sup>	5.0	5.76	31
5	1.15 x 10 <sup>8</sup>	1.7 x 10 <sup>9</sup>	7.9	7.20	6.0
6	8.00 x 10 <sup>7</sup>	9.0 x 10 <sup>7</sup>	11	8.64	5.5 x 10 <sup>-1</sup>
7	5.87 x 10 <sup>7</sup>	3.5 x 10 <sup>6</sup>	15	10.1	3.4 x 10 <sup>-2</sup>
8	4.50 x 10 <sup>7</sup>	8.5 x 10 <sup>4</sup>	21	11.5	1.3 x 10 <sup>-3</sup>

---

(a) For a work function of 4.5 volts

(b) For a 10 volt Ar<sup>+</sup> ion

velocity is,

$$v = \left( \frac{2qV_s}{M_i} \right)^{1/2} \quad (18)$$

The ion mass  $M_i = 1.660 \times 10^{-24}$  (M) gram. The atomic weight  $M$  for argon is 39.9. Thus for  $\text{Ar}^+$ ,  $M_i = 6.63 \times 10^{-23}$  grams =  $6.63 \times 10^{-26}$  kilograms. For a sheath potential of 10 volts  $v = 6.95 \times 10^5$  cm/sec. The corresponding transit times assuming a constant velocity is given in Table 1.

The field emission currents  $J_F$  are calculated for the various values of  $E_n$  and are given in Table 1. From the values of  $J_F$ , of average emission area, and of ion transit time, the corresponding values of field emitted electrons per ion are calculated and are presented in Table 1 and Figure 5. It is seen that (for  $\text{Ar}^+$  ions) according to this model, as many as 75 electrons per argon ion can be emitted from the cathode, and that the electron emission becomes effective when the ion is about 4 Å from the surface. When the ion mass is lower (such as hydrogen) the ion velocity is larger, and the transit time is shorter. Thus it is predicted that this individual-ion-field emission is less effective for lighter gases, but more effective for heavier ions. The calculated yield of electrons due to a  $\text{Hg}^+$  ion are shown for comparison in Figure 5.

A number of related problems should be considered. The space charge of the initial emitted electrons can produce a large electric field that can inhibit the rest of the field emitted electrons. The large electric field associated with the bipolar cathode sheath, however, can reduce the inhibiting effect of the emitted electron space charge. In addition, a minimal electron emission is required in order to be able to produce an inhibiting space charge field.

There is the necessity of explaining why this ion field emission effect is not apparent for the glow discharge. It is probably because the bipolar field is much less for the glow discharge than for the arc discharge. The current density for the glow discharge is many orders of magnitude less than for the arc discharge:

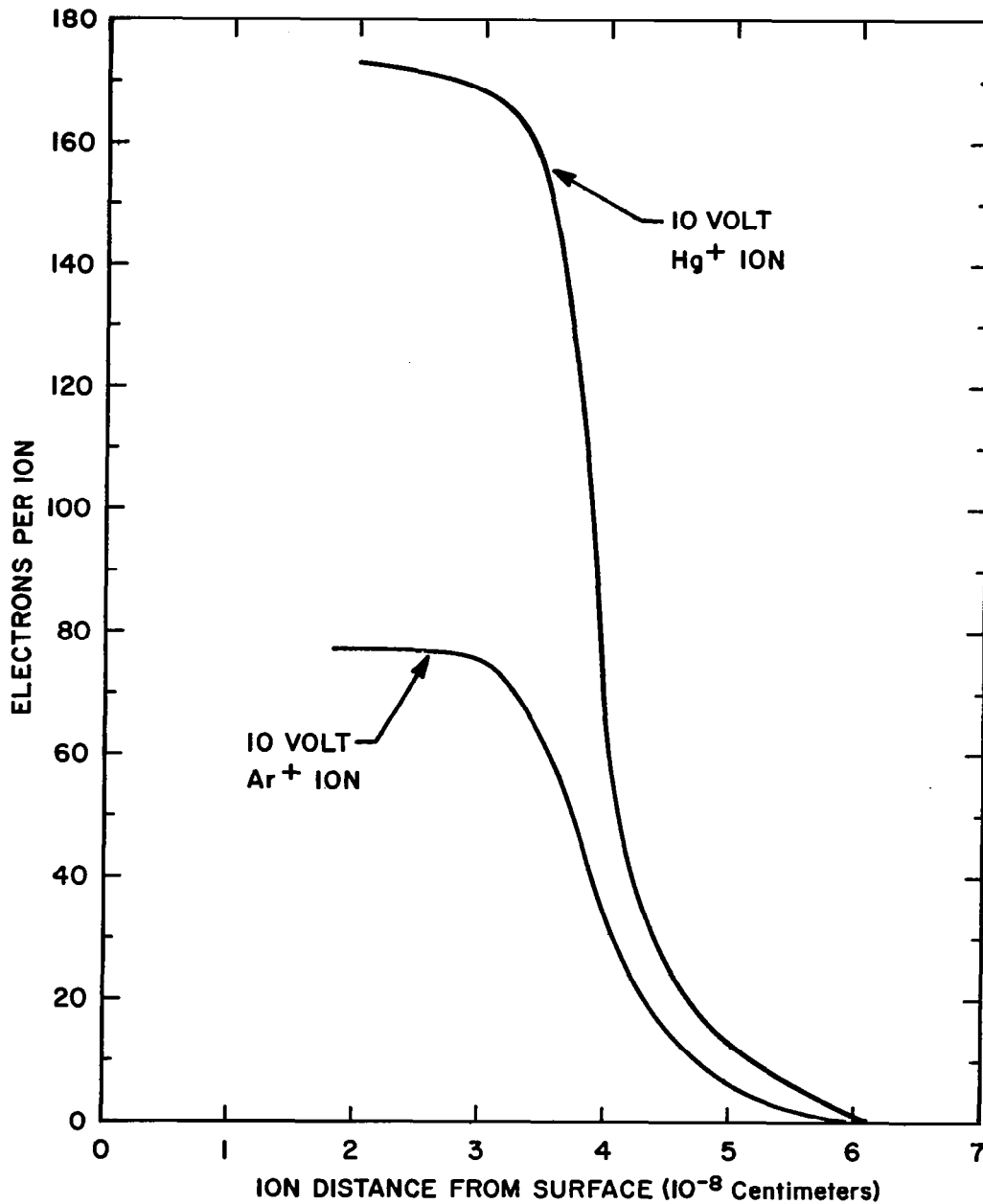


FIGURE 5.  
ELECTRONS EMITTED PER INCIDENT ION AS  
CALCULATED BY THE ION MICROFIELD  
EMISSION MODEL (USING AVERAGE VALUES).

The bipolar cathode field is therefore much lower and the emitted electron space charge field can prevent the escape of many cathode electrons.

If the positive ion is neutralized by one of the field emitted electrons, then the other field emitted electrons can still proceed to the plasma because of the strong bipolar cathode field. The determination of the neutralization distance is important since this can influence the actual electron emission.

Many of the problems of ion induced electron emission have been considered by Kisliuk<sup>7</sup> in conjunction with voltage breakdown.

#### 2.4 Arc Constriction

The constriction of arcs in plasmas is an important effect associated with magnetohydrodynamic propulsion systems and with magnetohydrodynamic power generators. This problem is related to the observation that for high currents, the plasma does not fill the available discharge channel. (The arc constriction is also frequently observed in sparks and in lightning strokes.) The same plasma constriction mechanism is probably operative in ball lightning. In those MHD structures where the arc is constricted, only part of the channel is filled with current carrying plasma, and the transfer of force between the neutral gas and the  $\mathbf{J} \times \mathbf{B}$  force is therefore not very efficient. Another important problem related to the arc constriction is due to the resulting concentration of energy flux at the anode, cathode, and insulator boundaries. The arc constriction is important in studying the interaction of the plasma with the electrodes, but it appears that the electrode interaction is not necessary to explain the observed plasma column constriction.

One of the most important reasons for damage to the electrodes is due to the fact that, for high currents, the arc operates as a contracted filament rather than as a diffuse plasma. This plasma contraction is undesirable for at least three reasons:

- (1) The small dimensions of the plasma (particularly at the anode or cathode) result in a large current density in the anode and cathode sheath and can result in a large sheath potential drop.

- (2) The constriction results in a large incident power density which can exceed the maximum power that can be tolerated at a concentrated spot without damage due to melting and evaporation.
- (3) The constriction of the arc reduces the interaction volume of the accelerated charges and the neutral gas. A large part of the gas can therefore flow with reduced acceleration.

This present study is aimed at gaining insight into the constriction mechanism and characteristics and could help in the reduction of arc constriction and the associated difficulties. Some of this material has been presented as a paper "A Study of Arc Constriction Processes" by S. Aisenberg and V. K. Rohatgi at the Seventh Symposium on the Engineering Aspects of Magneto-hydrodynamic, March 1966, but only with an abbreviated abstract because of space limitations.<sup>15</sup> A somewhat more detailed discussion will be presented here.

The mechanisms described here involve the balance between the input power to the plasma and the various modes of power loss. Considered here are the following modes of power loss:

- (1) Diffusion loss for low pressure plasmas,
- (2) Radiation loss for high density, high temperature plasmas,
- (3) Thermal energy loss for higher pressure plasmas, and
- (4) Convective energy loss due to the flow of cooler gas.

The various terms of the energy balance equation are dependent upon the arc radius: only for a definite plasma arc radius will there be equilibrium between the input power and the power loss. The analysis to be presented here is an extension of the Elenbaas-Heller equation.<sup>16</sup> The effect of self magnetic field pinching is neglected.

Since the relative importance of the various loss terms can not be specified without detailed information about the related physical constants, the analysis will proceed by taking limiting cases where only one loss term at a time is considered to be dominant. In this way, the general form of the dependence of the arc radius can be specified as a function of some of the plasma parameters.

An extension of the Elenbaas-Heller equation will be presented for the case of the (higher pressure) thermal arc. With this analysis it is possible to relate the radius  $R$  of the arc column to the axial potential gradient  $E$ , the thermal conductivity  $K$  of the plasma, and the electrical conductivity  $\sigma$ . The input power per unit volume (according to the Elenbaas-Heller equation)<sup>16,17</sup> is given by the product of the current density  $J$  and the potential gradient. If we assume that the energy is removed predominantly by thermal conduction, then

$$E \cdot J = - \operatorname{div} (K \operatorname{grad} T) \quad (19)$$

The term  $\operatorname{div} (K \operatorname{grad} T)$  is a negative term which depends upon the coordinates through the dependency of  $K$  upon the temperature  $T$  which in turn depends upon the coordinates. If the distance from the anode and cathode boundary is large enough so that we can neglect the axial flow of heat, then for cylindrical symmetry:

$$JE + \frac{1}{r} \frac{\partial}{\partial r} \left( rK \frac{\partial T}{\partial r} \right) = 0 . \quad (20)$$

With the substitution  $J = \sigma E$  (true for the plasma but not in the sheaths) one obtains

$$\sigma E^2 + \frac{1}{r} \frac{\partial}{\partial r} \left( rK \frac{\partial T}{\partial r} \right) = 0 . \quad (21)$$

The dependence of  $K$  and  $\sigma$  upon  $r$  is through the dependence upon  $T$  which in turn depends upon  $r$ .

If we assume a power law dependence for  $\sigma$  and  $K$  of the form

$$\sigma = \sigma_0 (T/T_0)^a \quad (22)$$

$$K = K_0 (T/T_0)^b \quad (23)$$

and let,

$$y = T/T_0 \quad (24)$$

$$\rho = r/R_0 \quad (25)$$

where  $T_0$  is the center temperature ( $r = 0$ ) and  $R_0$  is a characteristic distance or scale factor to make the radial coordinate dimensionless, then we get

$$\sigma_0 y^a E^2 + \frac{1}{R_0} \frac{1}{2} \frac{\partial}{\partial \rho} \left( \rho K_0 y^b \frac{\partial T}{\partial \rho} \right) = 0. \quad (26)$$

The terms  $\sigma_0$  and  $K_0$  correspond to the electrical and thermal conductivity at the center ( $T = T_0$  and  $r = 0$ ). If we set,

$$R_0 = \frac{1}{E} \left( \frac{K_0 T_0}{\sigma_0 (b+1)} \right)^{1/2} \quad (27)$$

we get the following equation;

$$y^a + \frac{1}{\rho} \frac{\partial}{\partial \rho} \rho \frac{\partial y^{(b+1)}}{\partial \rho} = 0. \quad (28)$$

Note that the selection of the scale factor of  $R_o$  is the one required to make the above equation dimensionless. The profile  $y = g(\rho)$  is unique (for given values of  $a$  and  $b$ ) so that there is a specific value of  $\rho_g$  for the value of  $y_g$  used to define the arc geometric dimensions. The corresponding geometric radius  $R_g$  is given by  $R_g = \rho_g R_o$  and is therefore proportional to the radial scale factor  $R_o$ .

The equation can be written in the form

$$\frac{1}{\rho} \frac{\partial}{\partial \rho} (\rho z) + z \left( \frac{a}{b+1} \right) = 0 \quad (29)$$

where  $z = y^{(b+1)}$

with the boundary conditions,

$$\frac{\partial y}{\partial \rho} (\rho = 0) = 0 \quad (30)$$

$$y (\rho = 0) = 1 \quad (31)$$

There are three special cases where  $\rho_o$  corresponding to the first zero ( $y = 0$ ) can be easily specified:

If  $a = 0$ , the solution is a parabolic function with a root of  $\rho_o = 2.0$

If  $\frac{a}{b+1} = 1$ , the solution is a Bessel function with a first root of  $\rho_o = 2.405$

If  $\frac{a}{b+1} = 2$ , the solution is a Spenke<sup>18</sup> function with a first root of  $\rho_o = 2.92$ .

The differential equation obtained by selecting the scale factor  $R_o$  to be,

$$R_o = \frac{1}{E} \left( \frac{K_o T_o}{\sigma_o (b+1)} \right)^{1/2} \quad (32)$$

is

$$\frac{1}{y} \frac{\partial}{\partial \rho} \left( \rho \frac{\partial y^{b+1}}{\partial \rho} \right) + y^a = 0 \quad (33)$$

$$\frac{\partial y}{\partial \rho} (\rho = 0) = 0 \quad (34)$$

$$y (\rho = 0) = 1 \quad (35)$$

and can also be written in the integral form;

$$y^{b+1} = 1 - \int_0^\rho \left\{ \frac{1}{\rho} \int_0^\rho \rho y^a (\rho) d\rho \right\} d\rho \quad (36)$$

This equation can be solved by assuming  $y(\rho)$  and then by numerically integrating twice to find  $y^{b+1}$ . This value of  $y^{b+1}$  can then be used to find a better value for the assumed  $y(\rho)$  and the integration can be repeated as needed. Because the double integration tends to reduce errors, the accuracy should be good and the convergence fast.

The actual geometric radius  $R_g$  of the arc is proportional to the characteristic distance  $R_0$ . If one describes the geometric dimensionless radius  $R_g$  by the distance for the temperature to drop to a fraction  $f_g$  of the central temperature, then  $y_g = T_g/T_0 = f_g$ . Since  $y = g(\rho)$  one can define  $\rho_g$  by

$$y_g = y(\rho_g) = f_g \quad (37)$$

with the inverse function

$$\rho_g = y^{-1} \text{ (at } y = y_g \text{)} \quad (38)$$

The actual geometric radius  $R_g$  is proportional to the radial scale factor  $R_o$  and is given by,

$$R_g = \rho_g R_o \quad (39)$$

For the thermal arc, the radial scale factor  $R_o$  has been shown to be described by;

$$R_o = \frac{1}{E} \left( \frac{K_o T_o}{\sigma_o (b + 1)} \right)^{1/2} \quad (40)$$

In the arc plasma near the cathode and anode sheaths, the electric field  $E$  becomes larger as it goes from the plasma to the sheath where there is less space charge neutralization. This suggests that near the sheath the radius of the plasma decreases. The constriction of the plasma near the electrodes is important because it will increase the power density to the electrode and will increase the damage to the electrode.

If one considers the correction due to the end loss terms and radiation terms, the effective value of  $E$  is reduced (the net power density generation is reduced) so that the radius  $R_o$  is increased. This last effect can become significant at about a distance of  $R_o$  from the electrode. Thus one may expect a constriction near the electrode together with a possible expansion just near the electrodes.

The previous analysis was developed for a thermal plasma where the energy loss is predominantly due to the thermal conductivity of the gas. In the accelerators of interest, the pressures are in the low-pressure (micron) range so that the plasma is not a thermal plasma (which is the case considered by the Elenbaas-Heller equation). It is possible to extend the energy balance equation to the low pressure case where diffusion loss should be considered dominant.

The rate of energy loss due to ion and electron diffusion is given by the product of the rate of electron and ion loss per volume  $-\text{div} (D \text{ grad } n_e)$  and of the effective energy loss  $q V_p$  per ion and electron pair, where

$$q V_p = q V_i + \frac{3}{2} kT_e + \frac{3}{2} kT_i \quad (41)$$

and  $V_i$  is the ionization potential. In general, the ionization potential energy is much greater than the thermal energy of the electron which in turn is greater than the kinetic energy of the ion.

It will be shown that the functional form of the various equations are the same for the low-pressure case (diffusion loss dominated) as for the thermal case (thermal loss dominated). The energy balance equation is

$$\sigma E^2 = -\text{div} (K \text{ grad } T) - q V_p \text{ div} (D \text{ grad } n_e) \quad (42)$$

where the first term on the right-hand side of the equation corresponds to the thermal loss, and the second term corresponds to the diffusion loss of ions and electrons. The electron (and ion) density is represented by  $n_e$ . It will be assumed that in the lower pressure plasma the thermal conductivity term becomes small compared to the diffusion terms and can be neglected. If one also assumes a cylindrical geometry and neglects end effects, then for the low pressure arc:

$$\sigma E^2 = -q V_p \frac{1}{r} \frac{\partial}{\partial r} \left( r D \frac{\partial n_e}{\partial r} \right) \quad (43)$$

where  $q V_p$  is the energy removed by each ion and electron diffusing out of the plasma. For plasmas of high electron density the diffusion coefficient  $D$  should

be the ambipolar diffusion coefficient  $D_a$  defined by

$$D_a = \frac{\mu_e D_i + \mu_i D_e}{\mu_e + \mu_i} \quad (44)$$

where  $\mu_e, \mu_i$  are the electron and ion mobility coefficients respectively and  $D_e, D_i$  are the diffusion coefficients for electron and ion respectively<sup>19</sup>. If the Debye length of the plasma is larger than the plasma dimensions the coefficient corresponding to "free diffusion" should be used<sup>19</sup>. The form of the equation is not changed. The electrical conductivity can be written as,

$$\sigma = qn_e \mu_e. \quad (45)$$

If it is assumed that  $D$  is independent of  $r$  then,

$$E^2 q \mu_e n_{e0} z = q V_p D \frac{n_{e0}}{R_0} \frac{1}{2} \frac{1}{\rho} \frac{\partial}{\partial \rho} \left( \rho \frac{\partial z}{\partial \rho} \right) \quad (46)$$

where  $\rho = r/R_0$ , and  $z = n_e/n_{e0}$ . The quantity  $n_{e0}$  is the electron density at the center of the arc.

If the characteristic radial scale factor is put in the form

$$R_0 = \frac{1}{E} \left( \frac{V_p D}{\mu_e} \right)^{1/2}. \quad (47)$$

Then the energy balance equation takes the form of the differential equation for the Bessel function;

$$\frac{1}{\rho} \frac{\partial}{\partial \rho} \left( \rho \frac{\partial z}{\partial \rho} \right) + z = 0. \quad (48)$$

For high electron densities the ambipolar diffusion coefficient  $D_a$  should be used. With the aid of the Einstein relation<sup>18</sup>,

$$\frac{D}{\mu} = \frac{kT}{q}, \quad (49)$$

it can be approximated by

$$D_a \approx \frac{kT_e}{q} \mu_i \left(1 + \frac{T_i}{T_e}\right). \quad (50)$$

For low pressures  $T_i \ll T_e$  and

$$\frac{D_a}{\mu_e} = \frac{kT_e}{q} \frac{\mu_i}{\mu_e}. \quad (51)$$

Thus the following result for the low pressure arc is obtained;

$$R_o = \frac{1}{E} \left( V_p \frac{kT_e}{q} \frac{\mu_i}{\mu_e} \right)^{1/2} \quad (52)$$

which is similar to the one for the thermal arc,

$$R_o = \frac{1}{E} \left( \frac{K_o T_o}{\sigma_o (b+1)} \right)^{1/2}. \quad (53)$$

Both the low pressure and thermal arc have the same dependence upon the E field. The analysis for both predict a constriction of the arc near the anode and cathode sheath.

It is possible to specify the arc geometric radius  $R_g$  as a function of  $I$  by means of the following equations for the low pressure arc:

$$R_o = \frac{1}{E} \left( V_p \frac{kT_e}{q} \frac{\mu_i}{\mu_e} \right)^{1/2} \quad (54)$$

$$R_g = \rho_g R_o \quad (55)$$

$$\bar{J} = \bar{\sigma} E = q \bar{n}_e \mu_e E \quad (56)$$

$$\bar{J} = \frac{I}{\pi R_g^2} \quad (57)$$

where  $\bar{J}, \bar{\sigma}, \bar{n}_e$  represent average values. When the above equations are solved for  $R_g$  as a function of  $I$ , the following is obtained;

$$R_g = I \frac{1}{\rho_g \pi q \left( \frac{\bar{n}_e}{p_o} \right) (\mu_e p_o) \left( V_p \frac{kT_e}{q} \frac{\mu_i}{\mu_e} \right)^{1/2}} \quad (58)$$

where  $\mu_e p_o$  is independent of the reduced pressure  $p_o$ . If it is assumed that the degree of ionization is essentially constant, then  $\bar{n}_e/p_o$  is constant and it is predicted that  $R_g$  is proportional to current.

A similar result can be obtained for the thermal arc. The following equations are applicable for this case:

$$R_o = \frac{1}{E} \frac{1}{(\sigma_o)^{1/2}} \left( \frac{K_o T_o}{b+1} \right)^{1/2} \quad (59)$$

$$R_g = \rho_g R_o \quad (60)$$

$$\bar{J} = \bar{\sigma} E = q \bar{n}_e \mu_e E \quad (61)$$

$$J = \frac{I}{\pi R_g^2} \quad (62)$$

with the following result

$$R_g = I \frac{\rho_g \frac{p_o}{\bar{n}_e}}{\pi q (\mu_e p_o)} \left( \frac{\sigma_o (b+1)}{K_o T_o} \right)^{1/2} \quad (63)$$

For a constant degree of ionization, the radius is predicted to be proportional to the current.

Based upon the previous models for the low pressure arc and for the thermal arc, it is possible to show that the current density decreases as the arc current increases. (This conclusion is based upon the arc energy balance equation plus a few assumptions.) A short proof is as follows: it was shown in the previous section that the arc radius was proportional to the arc current. Thus the arc cross sectional area is proportional to the square of the current and therefore the product of current density  $J$  and the arc current should be a constant.

It is possible to derive a negative resistance relationship between  $E$  and  $I$  for the low pressure arc and for the thermal arc, based upon the energy balance requirement. The case of the low pressure arc is given as an example. For the low pressure arc it was shown that

$$R_o = \frac{1}{E} \left( V_p \frac{kT_e}{q} \frac{\mu_i}{\mu_e} \right)^{1/2} \quad (64)$$

$$R_g = \rho_g R_o \quad (65)$$

$$\bar{J} = \frac{I}{\pi R_g^2} = q \bar{n}_e \mu_e E. \quad (66)$$

By combining the above equations it is possible to get

$$EI = \pi q \left( \frac{\bar{n}_e}{p_o} \right) (\mu_e p_o) \rho_g^2 \left( v_p \frac{kT_e}{q} \frac{\mu_i}{\mu_e} \right) \quad (67)$$

which shows that as  $I$  increases, the voltage gradient in the plasma decreases. This assumes that the degree of ionization remains constant. Negative resistance has been frequently observed in arcs.

Experimental verification of some of the analytical results can be demonstrated. For the case of the low pressure, diffusion loss dominated arc, it is deduced that the arc radius  $R$  should increase in proportion to the arc current  $I$ . The analysis predicts that the arc radius should vary inversely as the plasma potential gradient  $E$  in the plasma and therefore the arc should constrict near the anode and cathode sheaths where the potential gradients increase. For this analysis, the plasma conductivity is assumed to be constant and should be verified experimentally. A certain amount of verification is given by the reported results of measurements in low pressure arcs: they show that the arc spot width is indeed proportional to the arc current<sup>20,21</sup> and is in agreement with the analytical predictions. The data and the theory both predict that for this case the product of the current density  $J$  and the arc current should be constant.

When one considers the effect of a transverse magnetic field  $B$  on the plasma conductivity, the analytical model predicts that the radius should increase

as a function of  $B/p_0$  (where  $p_0$  is the reduced pressure). Measurements reported<sup>20</sup> for a low pressure mercury arc show that the radius increases as  $(B/p_0)^{1/3}$ .

A similar energy balance analysis was made for the high pressure arc where the dominant energy loss is due to gas thermal conductivity. It is found that the analytical functional dependence of  $R$  upon  $I$ , upon  $E$ , and upon  $B/p_0$  is similar to that for the previous case of the diffusion dominated arc. There appear to be no experimental data available to test the predictions for this situation.

For the case of a very high pressure plasma where the energy loss is predominantly due to radiation, it is predicted that the radius should be proportional to  $I^{2/3}$ . Experimental data to test this case have not been located.

The case of dominant convection cooling loss predicts that the arc radius should also increase as  $I^{2/3}$ . This result suggests that the current density should decrease as the arc current increases. Data reported by Milliaris<sup>22</sup> for a high pressure arc presumably cooled by convection and replotted in Figure 6, can be interpreted to show a variation of arc radius in proportion to  $I^{0.61}$  for several values of transverse magnetic field. This is in good agreement with the value of  $I^{2/3}$  predicted by the analysis described.

Further analytic and experimental study of arc constriction is recommended so that it might be possible to devise methods of reducing the constriction.

## 2.5 Analytical Study of Energy Transfer to Boundaries Using Continuum Theory

Some of the important processes associated with the transfer of energy and momentum to the electrodes have been investigated. In this section, a discussion is presented of the relative importance of various energy transfer contributions.

The various mechanisms that transport energy to the anode will be calculated in order to determine the dominant ones and to show that the energy transfer due to the electrons is much more important than the ion or neutral gas contributions.

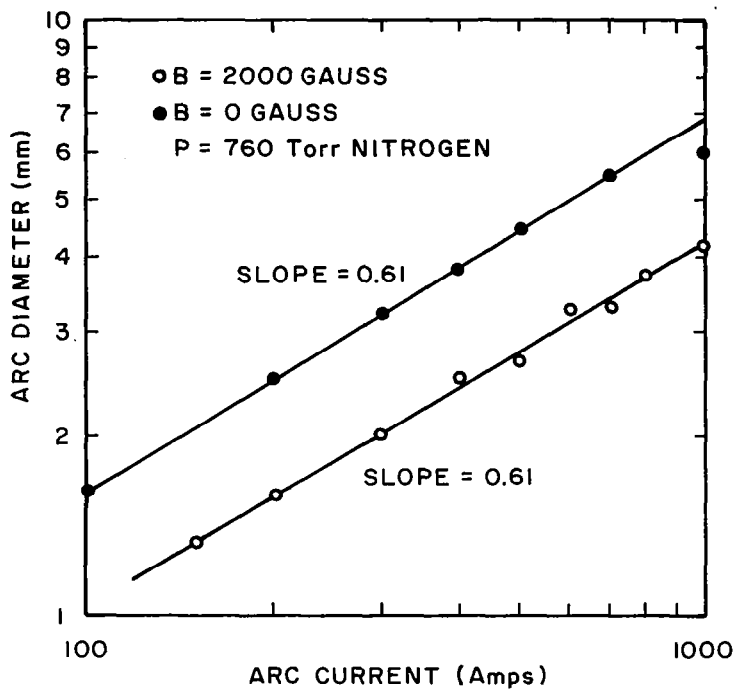


FIGURE 6.

ARC DIAMETER AS A FUNCTION OF ARC CURRENT FOR AN ATMOSPHERIC PRESSURE NITROGEN ARC. (FROM DATA OF MILLIARIS).

The energy contribution by electrons is calculated as follows: The random partial current density for a Maxwell-Boltzmann distribution (or any isotropic distribution function) is:

$$\Gamma = \frac{1}{4} n \langle v \rangle \quad (68)$$

where  $\Gamma$  is the number flowing per unit area per unit time,  $n$  is the number density and  $\langle v \rangle$  is the average velocity magnitude. For a Maxwell-Boltzmann distribution,

$$\langle v \rangle = (8q/\pi m_e)^{1/2} (m_e/m)^{1/2} (kT/q)^{1/2} \quad (69)$$

or numerically,

$$\langle v \rangle = 6.693 \times 10^7 (m_e/m)^{1/2} (kT/q)^{1/2} \quad (70)$$

where  $\langle v \rangle$  is in cm/sec,  $kT/q$  is the temperature in electron volts and  $m_e/m$  is the ratio of the electron mass to the particle mass. For atoms of molecular weight  $M$ ,

$$(m/m_e)^{1/2} = 42.69 (M)^{1/2} . \quad (71)$$

For argon  $M = 39.9$  so that  $(m/m_e)^{1/2} = 270$ . The energy transported to the anode for each electron flowing to the anode (at plasma potential) is given by;

$$W = q \left[ (2kT/q) + \phi \right] \quad (72)$$

where  $2kT/q$  corresponds to the kinetic energy transferred in the  $+x$  direction and  $\phi$  is the work function of the electrode. The electron charge  $q = 1.602 \times 10^{-19}$  coulomb and  $W$  is in Joules. The quantity  $q/k = 11,605^\circ\text{K/volt}$ . Assume that for electrons  $T = 10,000^\circ\text{K}$  and  $\phi = 4.5$  for tungsten. Then each electron transfers 6.2 electron volts to the surface. The energy flux density for electrons,  $S_e$ ,

is;

$$S_e = q \left[ (2kT/q) + \phi \right] (1/4) n (6.693 \times 10^7) (kT/q)^{1/2} \quad (73)$$

where  $S_e$  is in watts/cm<sup>2</sup>, and  $n$  is in cm<sup>-3</sup>. Figure 7 shows values of  $S_e$  calculated for various partial electron densities for the case of only electron kinetic energy ( $\phi = 0$ ) as well as for  $\phi = 4.5$  volts. It can be seen that energy flux in the 1 kw/cm<sup>2</sup> range can be reached in the electron density range of  $10^{14}$ /cm<sup>3</sup>.

If we consider the additional energy transported to the anode due to the voltage drop  $\Delta V_s$  across the electron sheath at the anode, then the energy transported by each electron is;

$$(2kT/q + \phi + \Delta V_s). \quad (74)$$

If we assume that the anode sheath potential drop is about equal to the ionization potential, then for argon;

$$\Delta V_s = V_i = 15.68 \text{ volts.} \quad (75)$$

The total energy per electron for this case is;

$$(1.92 + 4.5 + 15.68) = 22.1 \text{ volts.} \quad (76)$$

The energy flux for this case is also shown in Figure 7.

The neutral gas contribution has been studied and it can be shown that the kinetic energy transported to the anode by the random energy of the neutral gas atoms is small compared to the energy transported by electrons of the same number density. (This strong inequality is true if the gas is about 50% ionized and is weakened if the degree of ionization is small). For argon gas the energy flux is;

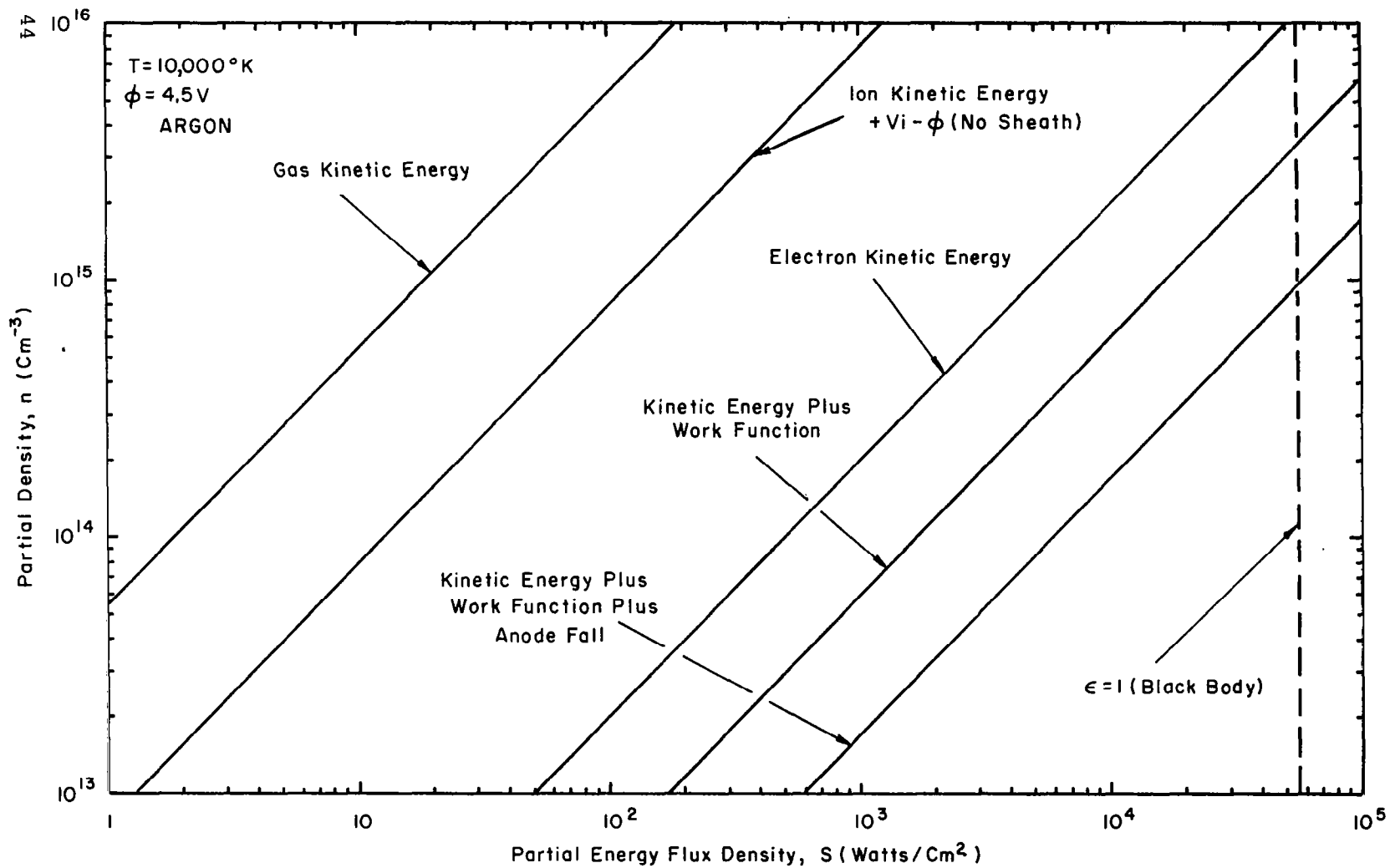


**FIGURE 7.**  
**ENERGY FLUX TRANSPORT TO ANODE BY VARIOUS PLASMA COMPONENTS.**

$$S_g = (2kT/q) (q/4) n \frac{(6.693 \times 10^7)}{270} (kT/q)^{1/2} \quad (77)$$

and is shown in Figure 7 for  $T_g = 10,000^\circ\text{K}$ . The gas kinetic energy contribution to the anode is seen to be small compared to the energy contribution of the electrons. Only if the gas atoms have significant tangential velocities near the anode surface (due to a process similar to "temperature jump"<sup>23</sup>) can the kinetic energy contribution of the neutral gas have a significant increase over the basic random energy component. The tangential (or axial) gas velocity in the center of the accelerator channel may be very large (for high specific impulse) but because of boundary drag effects, the tangential velocity near the surface can be reduced.

The velocity discontinuity at the surface (or one mean free path away from the surface) is given approximately by;

$$\Delta V = v_g - v_w = g_s \, dv/dx \quad (78)$$

where  $v_g$  is the gas tangential velocity,  $v_w$  is the wall velocity (assumed at rest),  $dv/dx$  is the gradient of the tangential velocity profile, and  $g_s$  is the "coefficient of slip"<sup>23</sup>. This value of  $g_s$  is approximately equal to the mean free path  $L$  and depends upon the surface accommodation coefficient. For lower pressures and large  $L$ ,  $v_g$  will be approximately the same as at the center. Unless the directed energy due to the velocity discontinuity is large compared to the gas temperature, the gas kinetic energy contribution will probably still be small compared to the electron contribution as shown in Figure 7. For the large average values of specific impulse that are desired for the accelerator however, the tangential kinetic energy in the center of the channel can be very large. Figure 8 shows the voltage equivalent of the kinetic energy for various atoms and ions as a function of specific impulse, S.I. (in seconds). This kinetic energy

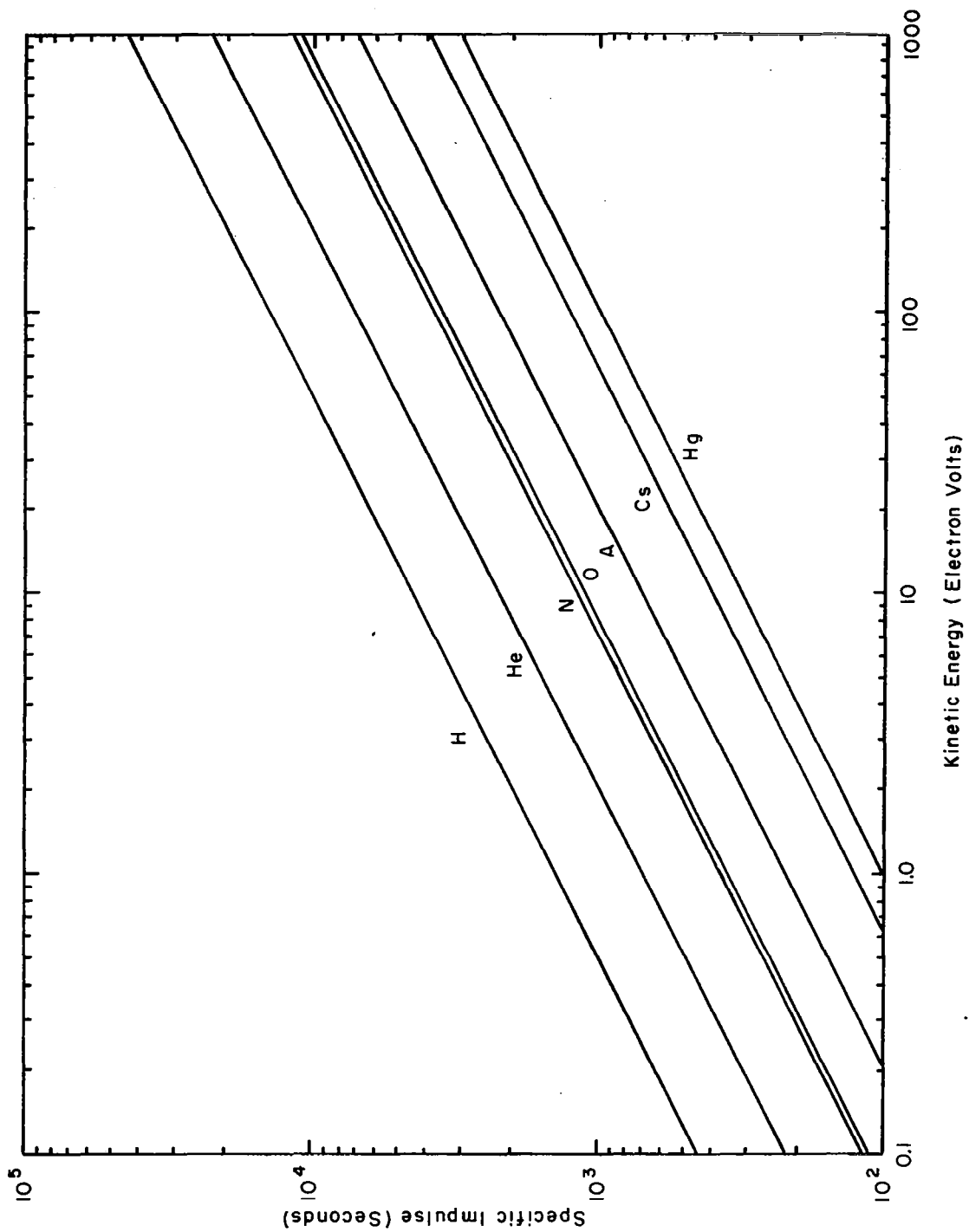


FIGURE 8.  
 KINETIC ENERGY AS A FUNCTION OF  
 SPECIFIC IMPULSE - FOR VARIOUS GASES.

is calculated from;

$$KE = \frac{m}{2q} v^2 = \frac{m}{2q} (S.I.)^2 (g)^2 \quad (79)$$

where  $g$  is the acceleration of gravity ( $980.7 \text{ cm/sec}^2$ ) and the KE is expressed in electron volts. As an example, for argon at a specific impulse of 3,000 seconds, the kinetic energy is about 180 volts.

If one considers the case:

$$\begin{aligned} n_- &= n_g \\ T &= 10,000^\circ\text{K} \\ \phi &= 4.5\text{V} \end{aligned} \quad (80)$$

and if the anode sheath potential drop and the tangential velocity are neglected, then for an argon plasma the energy transported by the electrons is 898 times greater than by the neutral gas. The presence of the anode sheath makes the energy transported by the electrons even larger. Only an unusually large tangential velocity can make the contribution of the neutrals comparable at the anode. The condensation energy of the atom on the anode is neglected since there is assumed to be no net accumulation. The effect of the energy accommodation coefficient of the atoms on the surface will reduce the gas kinetic energy transfer to even lower values.

The ion contribution to the energy transported to the anode is

$$\frac{2kT}{q} + V_i - \phi \quad (81)$$

for each ion where it is assumed that there is no sheath. If the anode is at plasma potential, the ion particle flux can be assumed to be the same as for neutrals of

the same density. The result is shown in Figure 7 for comparison with the other contributions. If the retarding ion sheath potential drop at the anode is considered, the positive ion current to the anode is reduced by many orders of magnitude and the ion current heating of the anode becomes even more negligible. Because of the ion sheath, the tangential force transported to the anode by ions is also considerably reduced.

Analysis of the radiation contribution to the energy transport shows that it is small for low pressure arcs. According to Spitzer<sup>6</sup>, the emitted intensity from a plasma at moderate temperature cannot exceed that from a black body at the kinetic temperature. For a low pressure arc the emissivity is low so that the energy coupled to the anode (and insulators and cathode) by radiation from the plasma is expected to be very small. The radiation energy flux from a body at temperature  $T$  is;

$$S_R = \epsilon 5.669 \times 10^{-12} T^4 \text{ watts/cm}^2 \quad (82)$$

where  $S_R$  is in  $\text{watts/cm}^2$ ,  $T$  is in  $^\circ\text{K}$ , and  $\epsilon$  is the emissivity (unity for a black body) Figure 7 shows  $S_R$  computed for  $T = 10,000^\circ\text{K}$  and  $\epsilon = 1$ . Since the actual emissivity for the low pressure plasma is expected to be much less than unity, the contribution by radiation can be neglected. The gas pressure in typical accelerators can be shown to be in the micron pressure range.

The following summarizes the situation for energy transport to the cathode. The energy transported to the cathode spot appears to be primarily through the ion current component. Because of the electric field at the sheath edge, the ion current flow is much greater than the neutral gas flow (unless the degree of ionization is very low). At the same time the internal energy of the ion plus the energy gained in the cathode sheath fall is much greater than the kinetic energy of the gas atoms. Thus the energy flux density to the cathode due to positive ions is much greater than the neutral gas energy flux (if the degree of ionization is sufficiently high).

The electrons that are emitted will transport energy to the plasma and can contribute energy to the cathode spot only through ohmic heating in the electrode material itself. Since the voltage drop in the electrode itself is small the power contributed by ohmic heating is small. In fact, the thermionic electron emission component of the arc current actually cools the cathode by an amount related to the cathode work function.

Energy transport to the cathode by excited atoms is difficult to compute unless the density of excited atoms can be specified. If the density of excited states is about 1% of the ground state (it will probably be much less) and if the excitation energy (about 10 eV) is only about one order of magnitude greater than the kinetic energy ( $T = 10,000^\circ\text{K}$ ), the energy flux due to excited states is expected to be smaller than the energy flux due to neutral gas kinetic energy.

The only way that appreciable power can be delivered to the cathode is through positive ion current to the cathode. Ohmic heating in the cathode spot neighborhood, plasma radiation, excited atoms, and thermal energy of the gas atoms can also contribute energy to the cathode but probably not a significant fraction. The cathode electron current actually delivers energy to the plasma and not to the cathode.

The power density transferred to the cathode spot by positive ions is appreciable. As an example, if one assumes a typical value of cathode spot total current density of about  $10^4$  amp/cm<sup>2</sup>, a cathode sheath drop of about 10 volts, a ratio of  $J_+/J_{\text{total}} \approx 10\%$ , an ionization potential of about 15 volts, a work function of about 4.5 volts, and a thermal energy of  $10,000^\circ\text{K}$ , then the power density delivered to the cathode spot is about  $2 \times 10^4$  watts/cm<sup>2</sup>.

An important part of the  $J \times B$  electrode problem is the question of what part of the cathode current is due to electron emission and what part is due to ion collection. This current partitioning is important in the energy balance calculation. In addition, the collection of ions at the cathode is important from the momentum transfer point of view because each ion collected by the cathode will

deliver a portion of its tangential momentum. The tangential energy component will add to the cathode heating. The performance of the unit as an accelerator will depend upon both the tangential and perpendicular momentum lost by the ions flowing to the cathode.

It appears that the ion current to the cathode spot is a key problem because 1) it transports significant energy to the cathode spot, 2) it transports significant tangential and perpendicular momentum to the cathode, and 3) it is necessary for all prominent physical models used to explain electron emission from the arc cathode spot.

A detailed discussion of the role of positive ions in electron emission was given in Section 2.3.

## 2.6 Arc Retrograde Motion

As part of the investigation of the tangential plasma velocity along electrodes it was found necessary to study briefly the phenomena of retrograde motion.

Essentially, the concept of retrograde motion corresponds to the observation that an electric arc in an external magnetic field  $B$  will move in a direction perpendicular to both the current and the magnetic field. The motion of the arc is expected in view of the Lorentz force that acts upon a charged particle moving in a magnetic field. However, it is observed that under low pressure conditions the arc moves in the direction opposite to that expected from the Lorentz forces. The arc motion in this case is called Retrograde Motion, and can not be explained in terms of the opposite charges or opposite velocities of the positive ions and electrons.

If one is to feel that the plasma arc is understood, it is necessary to explain the phenomena of retrograde arc motion. Retrograde arc motion has been studied as far back as 1903<sup>24</sup> and by many subsequent researchers<sup>25</sup>, but no really satisfactory explanation has been presented.

To be briefly outlined here is a model which has been developed to explain the retrograde motion in terms of the plasma growth into regions where the magnetic field is larger. Thus the retrograde arc motion can be described as a process similar to phase velocity rather than actual retrograde particle velocity. The essential feature of this model for retrograde motion is that the diffusion and mobility loss of electrons and ions (ambipolar diffusion) is reduced by the presence of large magnetic fields. On the retrograde side of the arc, the self magnetic field is in the same direction as the external field and is in the opposite direction in the Lorentz side of the arc. The Lorentz force model predicts that the arc will move into regions where the magnetic field is weakest. (This can also be seen on the basis of the elastic magnetic flux model). The plasma growth model on the other hand predicts that the arc will grow in the direction where the magnetic field is largest - this prediction is in agreement with the observations of retrograde motion.

It thus appears that many of the features of retrograde motion (as well as the actual direction) can be explained by the model of plasma propagation growth in the direction of large total magnetic fields where the ambipolar diffusion is reduced.

The retrograde motion therefore does not correspond to retrograde motion of the plasma particles and therefore one need not consider the possibility of retrograde tangential electrode drag.

### 3. EXPERIMENT

During the course of this investigation various experiments were conducted to study the physics of plasma surface interactions in the case of a magnetically accelerated arc. An investigation was made of some of the problems related to the transfer of tangential momentum and to the constriction of arc at the electrodes. Most of the emphasis in this study was placed on the electrode drag measurement due to its relative importance in the development of plasma accelerators. The presence of a tangential force is a measure of the transfer of momentum by ions, electrons and gas particles when they collide with a surface. The basic concept for the drag measurement was suggested by Dr. K. Thom and his co-workers.

Basically two types of electrode configurations were used in these experiments: 1) the electrode drag measurements were made with electrodes such that the magnetic field was normal to the flow of current in the entire channel and 2) the measurement of arc dimensions and voltage dependence on the magnetic field at the cathode were made with electrodes where only the cathode sheath region was at right angles to the B field.

In the drag experiment, as in the case of a  $J \times B$  accelerator, since the magnetic field acts on the electrode sheaths as well as on the plasma, the sheath effects could not be separated experimentally from the plasma effects. Also the geometry of the apparatus did not permit a direct observation of the effect of magnetic field on the size of the arc spot which plays an important role in the understanding of the electrode phenomena. The second experiment was therefore performed in which the magnetic field interacted only with the cathode region. The flow of current in the plasma and the anode sheath were made parallel with the magnetic field. This electrode arrangement offered a direct visual observation of the size of the cathode spot. Again since the flow of current in the plasma and at the anode were parallel to the B field, the change in the tube characteristics were

related mainly to the change in the cathode region due to the B field. It was thus possible from this experiment to study the arc constriction and the dependence of the cathode voltage upon the B field and gas pressure. The details of these experiments together with the results are given in the following sections.

### 3.1 The Electrode Drag Measurement

In this section is described the design of the apparatus and necessary instrumentation developed to measure the transfer of tangential momentum from an arc to the electrodes under the action of a magnetic field. Much of the analytical work and design considerations required for this experiment have already been presented in the Summary Report<sup>26</sup>. For example, the analysis of the expected modes and magnitudes of the transfer of energy from a given plasma to the electrode proved very valuable in the design of the main arc apparatus and of the auxiliary instruments used to measure the small torque on the rotating electrode.

The early results of this experiment have been described in a brief preliminary publication<sup>27</sup>. Further results will be described in Section 3.2.

Figure 9 shows the layout of the apparatus for the measurement of tangential electrode forces. The rotary electrode was made of molybdenum (and also of copper) rod about 10 cm long and having a 2 cm diameter. The active electrode however, was only 2 cm in diameter and 1 cm long. The arc current to this electrode was fed through a liquid mercury pool. A thick layer of low vapor pressure silicon oil was provided on the mercury surface to suppress the Hg vapor contamination in the arc plasma. To reduce the homopolar and electromagnetic forces in the liquid pool commutator, a wedge shaped contact was designed (Figure 9, Detail A) to force the current to flow parallel to the magnetic field in the Hg pool. Also the current into the electrode was injected at the same radial point at which it left the electrode thus minimizing the homopolar forces.

The rotary structure was supported on a Bendix torsion spring, so that the tangential force on the electrode was measured in terms of the spring deflection. The small angular displacements of the spring were detected by a multiple coil

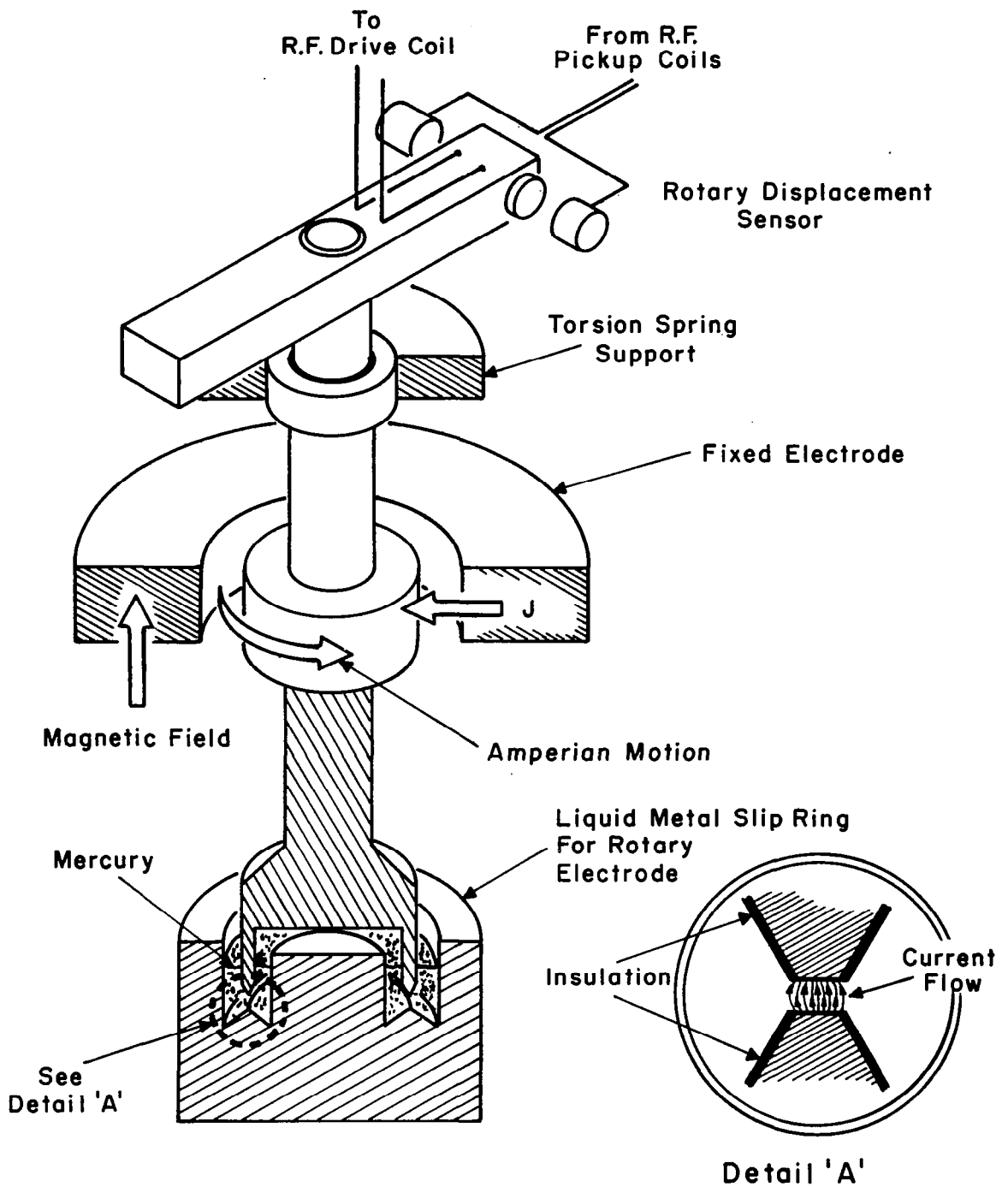


FIGURE 9.  
 SCHEMATIC OF ROTARY ELECTRODE STRUCTURE FOR THE  
 MEASUREMENT OF TANGENTIAL ELECTRODE FORCES.

R.F. transducer. The details of the torsion balance are described in Section 3.1.2.

The fixed electrode of the plasma generator consisted of a water cooled copper ring, 1 cm thick and about 9 cm in diameter with a 3 cm diameter hole in the center. This was located symmetrically around the rotary electrode so that the arc ran radially in a gap of 0.5 cm long and 1 cm wide. By using ring electrodes with different openings, the length of the plasma could be varied conveniently. Provision was made so that the center rotary electrode could be used as a cathode or as an anode.

A magnetic field parallel to the axis of rotation was generated with a water-cooled conventional air core electromagnet, located outside the vacuum chamber. A Helmholtz coil structure was adopted to create a uniform field in the test region. The magnet was capable of producing fields up to 2 kilogauss for continuous operation and above 3 kilogauss for a short period.

3.1.1 Improved insulators for arc electrodes. -- Early in the experiment while measuring the electrode drag, it was seen that often the arc locked at the boundary of an electrode and burnt the insulation. The cavity thus formed was a favorable site for subsequent locking of the arc. The arc voltage and the tangential forces were extremely high and inconsistent whenever the arc was anchored to these spots. On the other hand, with a freely running arc, the data was reproducible.

Initially a solution to this problem was sought by applying the commercially available dielectric coatings. Tests were conducted with several epoxies, mica, abestos and ceramic bodies including alumina films formed by plasma-spray techniques. Although the performance of the device varied slightly with these coatings, there was no outstanding improvement in the results. In general, high temperature ceramics were found to be somewhat better, but the overall gain was not appreciable in view of the difficulties in their preparation.

These experiments revealed that the failure of the insulation and hence of the device was due to the excessive thermal stresses at the point where the arc

was anchored. A critical study of the damaged electrodes showed that the erosion of material was more pronounced for the dielectric because the arc heat could not be conducted away due to low thermal conductivity of the dielectric. This also explains why the ceramic insulators, capable of withstanding higher temperatures, survived longer compared to the epoxies and plastics.

A new concept of metallic insulator was then developed which yielded a very satisfactory solution to this problem. These insulators extended the operating life of the device several fold and also reduced the scatter in the experimental measurements. A technical paper describing this technique has been published<sup>5</sup>. This method will be described briefly here.

Figure 10 shows the schematic arrangement of the electrodes together with the metallic insulators. The metallic shields were electrically insulated from the main arc electrode by thin layers of high temperature ceramic. The dielectric in this case was a water base refractory cement<sup>28</sup> (SAUEREISEN #P-78) recommended for use up to 3000°F. The thickness of the coating varies from 0.5 to 1 mm. Satisfactory results were obtained with uniform thin coatings (about 0.5 mm) which were free of air voids.

The metallic shields were made of heavy metal blocks having high thermal capacity. Initially shields of aluminum were tried to take advantage of the low density and ease of fabrication. However, its low melting point ( $T = 660^{\circ}\text{C}$ ) imposed a limitation on its life, and the erosion damage was shifted from the ceramic to the aluminum shield. Replacing the aluminum with molybdenum shields resulted in a much superior system. Forced cooling of these shields was not practical nor necessary in the present apparatus. It is, however, believed that water cooled copper shields should be equally satisfactory (or perhaps even better) due to the high thermal conductivity of copper.

These electrodes were used for arcs up to 100 amps in argon and helium. Electrostatic biasing of the metallic shields on the cathode electrode to deflect

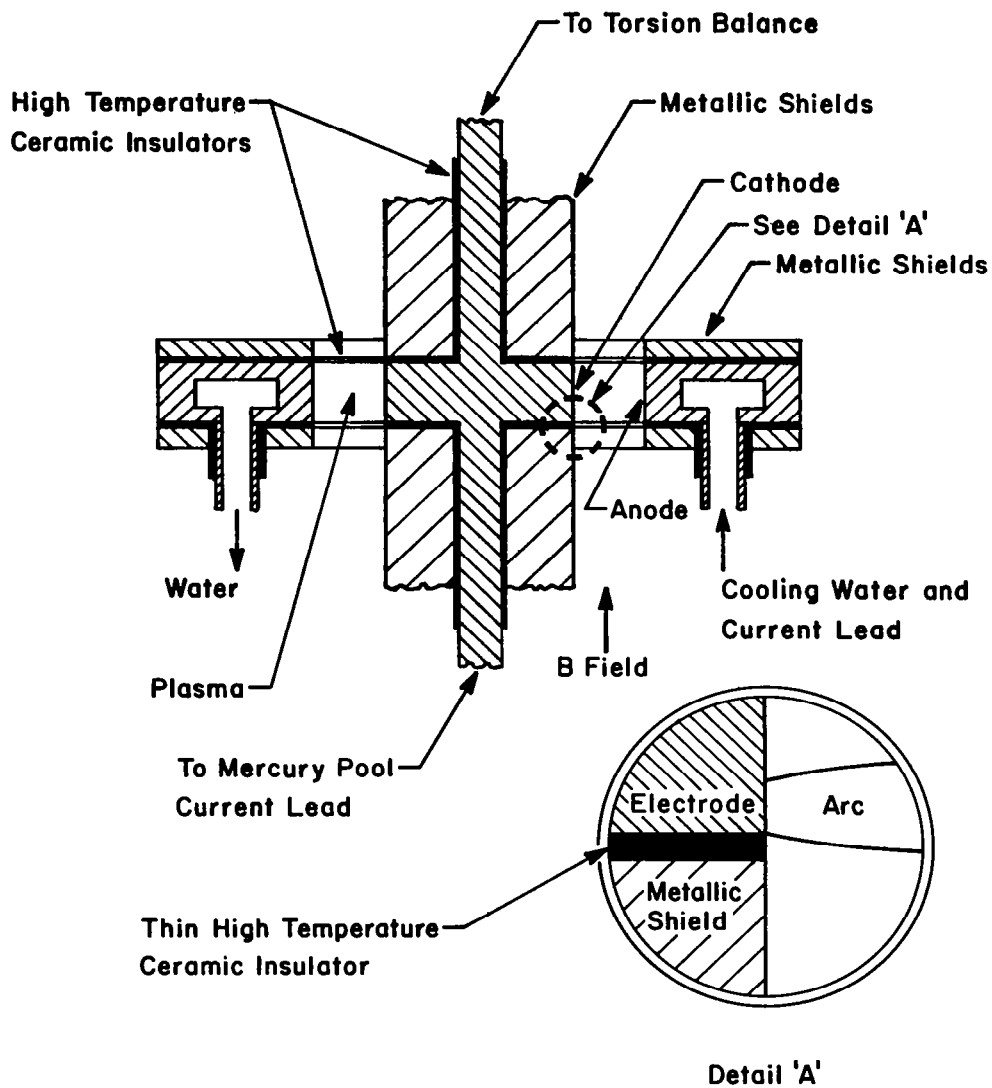


FIGURE 10.  
 METALLIC INSULATORS FOR ARC ELECTRODES.

the electrons did not influence the performance of the device or the arc characteristic. For most of the operation the electrode shields were kept floating. A floating potential of about 0.7 volts was recorded on the shields of the cathode electrode.

3.1.2 Drag measurement instrumentation. — A sensitive transducer was required to measure small deflections corresponding to the small forces on the electrodes. A Bendix torsion spring, having no backlash, no starting friction, and no lubrication requirement was preferred to a regular bearing for this purpose.

Figure 11 shows the circuit diagram of the oscillator and phase sensitive demodulator for detecting small displacements of the transducer. An R. F. signal of 2.5 MC was supplied to the transducer driving coil which was coupled through a differential transformer connection to the R.F. pickup coils. The locations of R.F. drive and pickup coils are indicated in Figure 9. The signal from the pickup coils, after demodulation, was recorded on a strip chart recorder.

The calibration of the balance was made with known weights and lever arms each time the apparatus was dismantled and reassembled. The torque sensitivity of the instrument was about 30 mV per gm-cm, and was symmetrical and linear up to 3 gm-cm.

A typical torque measuring sequence is shown in Figure 12. Initially when the B field was turned on (with the arc off) the transducer assumed a new zero position. This displacement was due to the magnetic property of the spring material and was proportional to the direction and magnitude of the B field. The oscillatory nature of the signal demonstrated the free mechanical response of the transducer and the freedom from friction. The damping time (about 3 sec.) depends on the spring constant and the liquid pool at the bottom of the rotary electrode. The sensitivity and the response of the transducer could be checked at any time during the experiment by observing the damping of the signal.

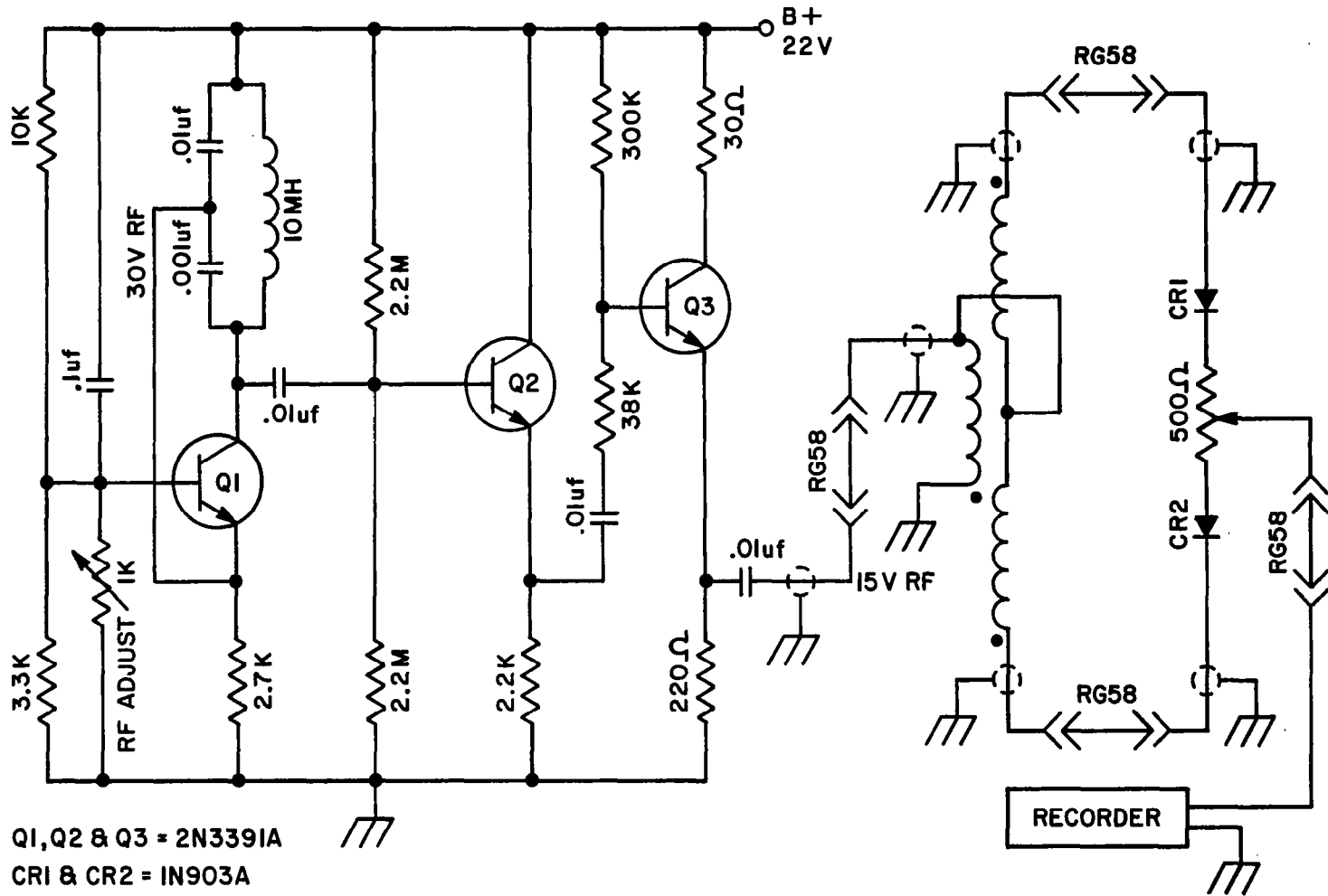
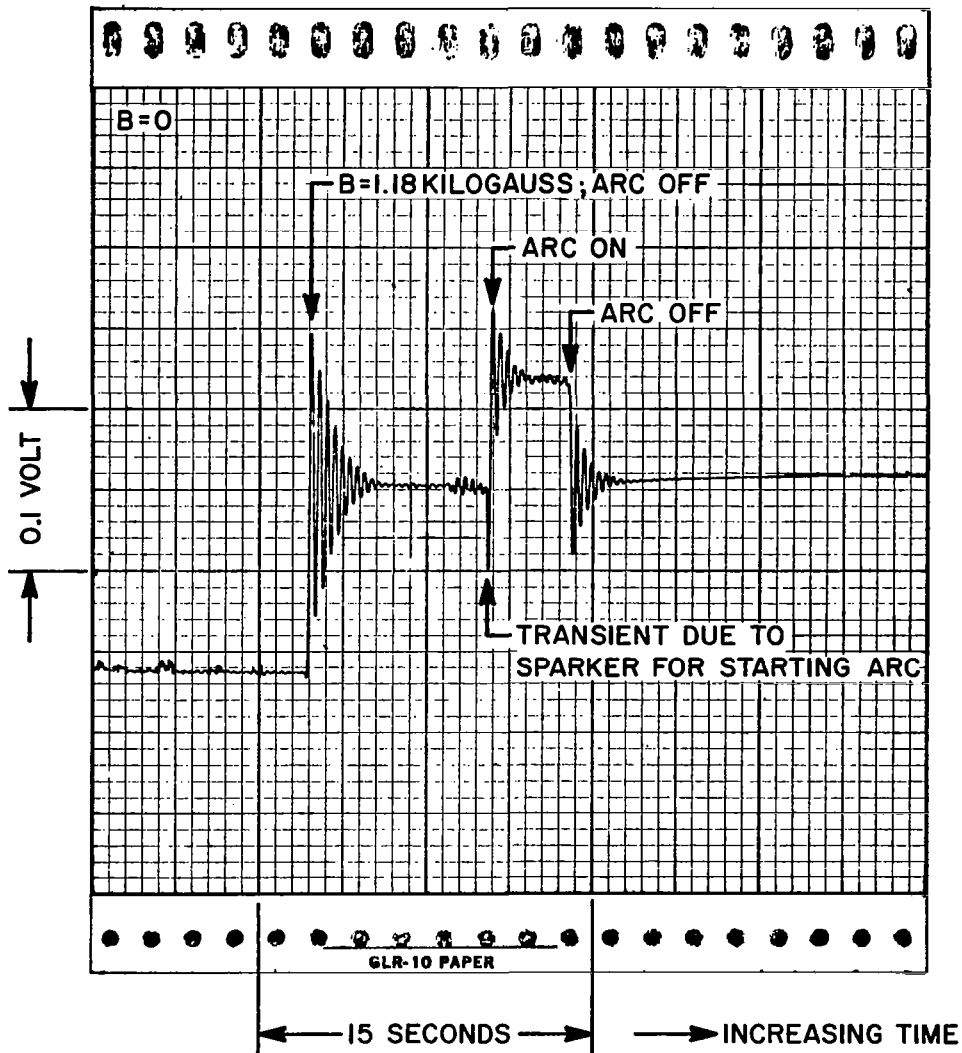


FIGURE 11.

CIRCUIT DIAGRAM OF RF OSCILLATOR AND PHASE SENSITIVE DEMODULATOR.



NOTE: TANGENTIAL FORCE ON COPPER CATHODE  
 RADIAL GAP: 1 CENTIMETER  
 50 AMP ARC IN 0.2 TORR OF ARGON

FIGURE 12.

TRANSIENT RESPONSE OF TRANSDUCER SYSTEM WHICH  
 MEASURES THE TANGENTIAL ELECTRODE FORCE FOR  
 AN ARC IN A TRANSVERSE MAGNETIC FIELD.

After the B field was on, the arc was started when the transducer trace became steady. The tangential force exerted on the electrode due to the  $J \times B$  force was determined from the displacement of the transducer from the new zero position. Due to the effect of plasma heat on the Bendix spring the torque measurements were made in the ballistic mode, allowing adequate time for the apparatus to cool down between the tests.

### 3.2 Analysis of Results of Drag Study

This section deals with the results of the tangential force measurement as a function of magnetic field and of the gas pressure. The preliminary measurements of the tangential electrode forces have been described elsewhere<sup>27</sup>. The drag forces on cathode and anode were measured by operating the central electrode as cathode and anode respectively. The tests were conducted with argon and helium gases.

Some results are illustrated in Figures 13 and 14 where the measured tangential force is shown as a function of magnetic field for fixed arc currents and fixed gas pressures in argon and helium. The cathode force due to ion current drag is deduced by assuming that the neutral gas component at the cathode is the same as the anode drag. (This assumption should be examined further because the boundary layers at the anode and cathode may be very different).

These results show that:

- (1) The measured tangential force was in the amperian direction and, as expected, the sign of the force changed when the B field was reversed.
- (2) The sign of the force was different for the anode because the sign of the current flow was reversed.
- (3) There is a pronounced threshold in the electrode force as a function of the magnetic field.

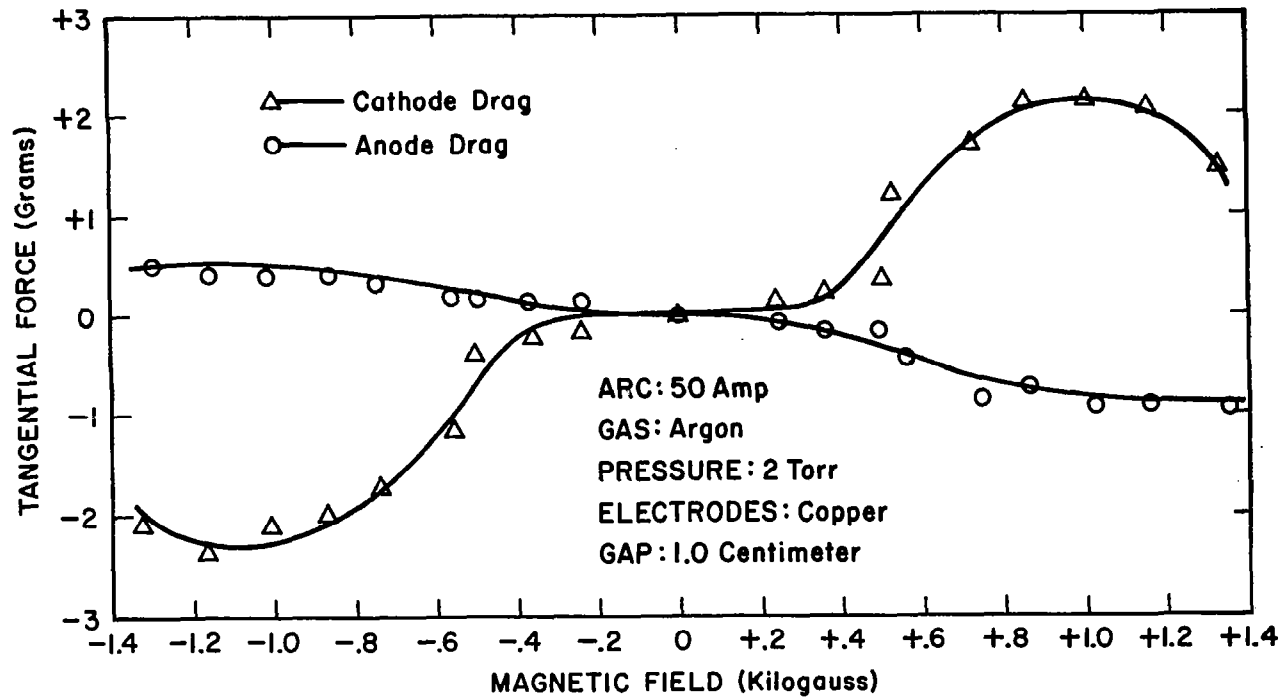


FIGURE 13.

DRAG FORCE ON ELECTRODES OF A  $J \times B$  ARC  
AS A FUNCTION OF MAGNETIC FIELD (AT LOW PRESSURE).

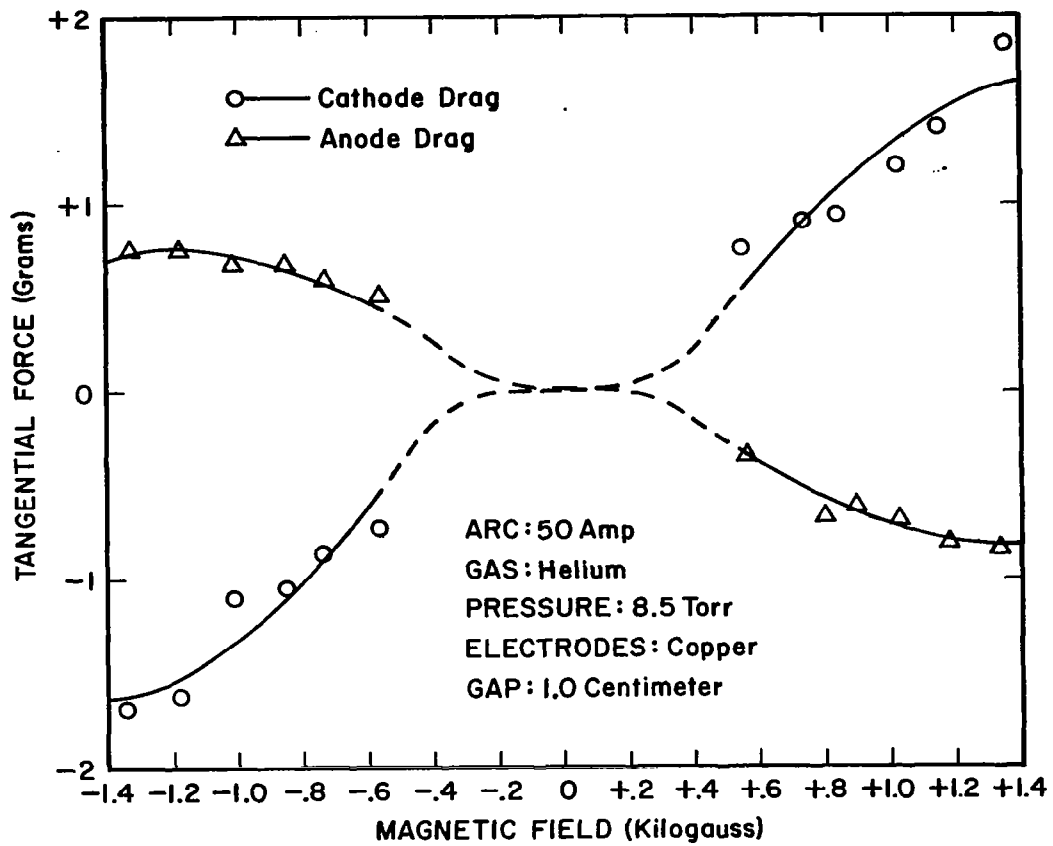


FIGURE 14.  
 ELECTRODE DRAG FORCE vs MAGNETIC FIELD  
 IN HELIUM.

- (4) The fact that force thresholds are measured demonstrates that strong homopolar forces are not significant.
- (5) In the range studied, the maximum cathode force was about 2.6 times larger than the maximum anode force.
- (6) If it can be assumed that the momentum transfer to the anode is predominantly due to the neutral gas atoms, there appears to be a threshold in the electrode drag by the neutral gas components.
- (7) At large B fields, the drag force at both electrodes appear to saturate and to then decrease for further increase in B field.
- (8) The threshold for anode drag appears to be larger than the threshold for cathode drag.
- (9) The cathode force was as large as 24% of the input force driving the plasma, and the anode force was as large as 13%.
- (10) The deduced ion current drag component was larger than the neutral gas component, and in the range measured, was about 16% of the plasma driving force.

The tangential force on an electrode is proportional to the tangential velocity, to the perpendicular particle current flow, and to the tangential momentum accommodation coefficient. The observation that the tangential force at the cathode was larger than the anode force indicates that the positive ion current flow to the cathode is capable of transferring an appreciable tangential force to the cathode. The observation of the threshold in the electrode force components indicates that there may be thresholds in at least one of the following: the tangential velocity, the perpendicular particle current flow of the ions and neutrals, or in the momentum accommodation coefficients. When the tangential velocity of the ions is determined, it should be possible to compute the positive ion current to the cathode for comparison with the total arc current.

The effect of gas motion on the drag force was investigated by putting shields around the plasma chamber. Within the accuracy of the experiment, the data with and without the shields demonstrated that the electrode force was unaffected by the modification in the axial gas flow away from the electrodes. It may thus be concluded that the force transferred to the electrode was predominantly related to the interaction of the arc root at the electrode, and not due to the motion of the gas.

The dependence of threshold B field for cathode drag on arc current is plotted in Figure 15. These data show a power law dependence of the arc current on the threshold B field with an exponent of about 2/3.

The cathode drag force was also measured as a function of gas pressure. The results of this observation are plotted in Figure 16, which shows that the drag force at lower pressures is about twice the force at higher pressures in the range studied. In general the drag force was a weak function of the gas pressure. The low drag at higher pressure can perhaps be explained in terms of higher gas friction and lower particle velocities.

### 3.3 Deduction of Current Partitioning at the Cathode

The problem of current partitioning at the cathode spot is of interest in the development of  $J \times B$  accelerators and magnetohydrodynamic power generators, because of the strong interaction of the arc with the electrodes. From the measurement of tangential force it is possible to calculate the ion current component at the cathode. The tangential ion force  $F$  on the cathode in terms of arc current  $I$  can be expressed as,

$$F = \sigma (mv) \frac{I}{e} f \quad (83)$$

where,

$\sigma$  = tangential momentum accommodation coefficient,

$f$  = fraction of total current that is carried by positive ions,

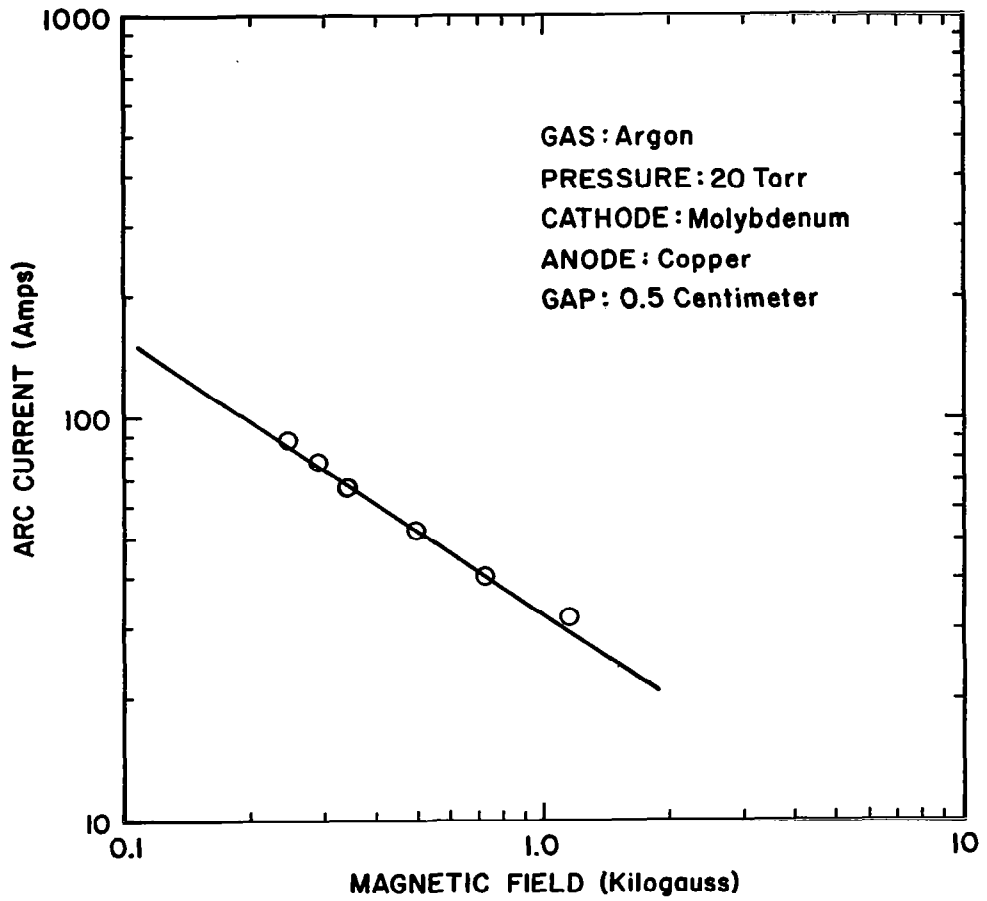


FIGURE 15.  
DEPENDENCE OF THE THRESHOLD B FIELD  
FOR CATHODE DRAG ON THE ARC CURRENT.

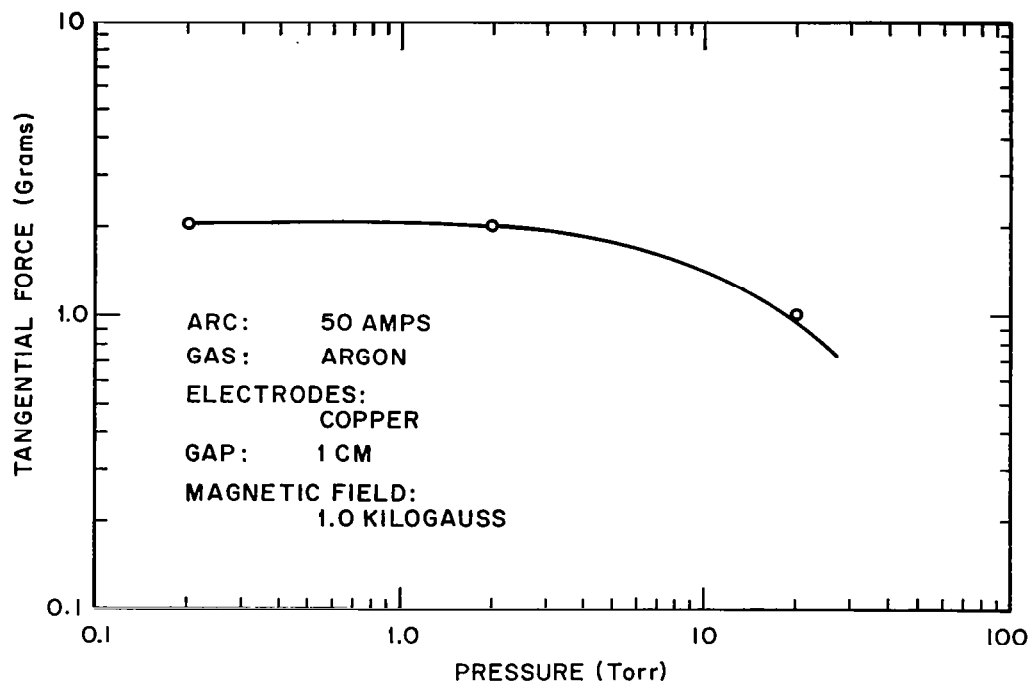


FIGURE 16.  
DEPENDENCE OF CATHODE DRAG ON GAS PRESSURE.

m = mass of the ion,  
v = velocity of the ion, and  
e = charge carried by the ion.

If the quantities, F and I are determined by the experiments, Equation (83) can be used to calculate the positive ion current component f in the arc, provided that v and  $\sigma$  are known and that the ions are singly charged. Based upon the results of Lin<sup>29</sup> and of Lehnert<sup>30</sup> the ion velocity in this calculation may be taken to be the Ionization Limit velocity.

To evaluate the positive ion current fraction f at the cathode from this experiment, a value must be assigned to  $\sigma$ . If the surface and ion temperatures are low, as in the case of an electrostatic probe, it is customary<sup>31</sup> to assume that all the incident particles will be trapped by the surface so that  $\sigma$  is equal to unity. There is however, no evidence that the value of  $\sigma$  will remain close to unity in a constricted arc where the surface temperatures and the energies of the incident ions are very high. The interaction between the gas and the solid depends upon the surface films and the roughness of the target surface as well as on the type and energy of the incident particle<sup>8</sup>. Unfortunately no definite information is available regarding  $\sigma$  for a situation such as considered here. According to Boule<sup>32</sup> if it is assumed that the transfer of momentum between the ion and the target takes place in a single collision, then one can very roughly estimate the momentum accommodation coefficient in terms of the masses of the colliding particles. The coefficient  $\sigma$  can be estimated from the expression<sup>26</sup>,

$$\sigma (2 - \sigma) = \alpha \quad (84)$$

where,

$$\alpha = \frac{2m_1 m_2}{(m_1 + m_2)^2} \quad (85)$$

is the energy accommodation coefficient as given by Baule, and  $m_1$  and  $m_2$  are the masses of the two colliding particles. The simple, single free collision model of Boule, however, does not seem to be quite satisfactory to estimate the accommodation coefficients of a gas ion on the electrode surface in view of the presence of other strongly influencing parameters. It will be perhaps more instructive to calculate the ion current fraction by assigning a maximum accommodation coefficient which will then give the lower limit of the current partitioning at the cathode.

If in the present example, we therefore assume a maximum value of  $\sigma$  of unity (corresponding more closely to the case of an electrode which is rough on a microscopic basis) it is then possible to calculate the positive ion current component at the cathode using the drag force measurements. Table 2 shows the deduced positive ion current fraction at the copper cathode in argon and helium arcs. It is to be mentioned here that these estimates are subject to some error due to the uncertainty in the accommodation coefficients and also the uncertainty in the use of ionization limit velocities. It is, however, interesting to note that this method yields the ion current fraction at the cathode which is of the same order of magnitude as suggested by Lee<sup>33</sup> and is also consistent (within a factor of 2) with the energy balance conditions at the cathode. The ion current at the cathode as determined from the drag measurements is expected to be higher than shown in Table 2 due to expected lower values of  $\sigma$ .

From this study it can be concluded that the drag forces at the electrodes are observed here represent a real effect and show the parts played by ions, electrons and the neutral gas particles in the transfer of momentum to the arc electrodes.

TABLE 2  
POSITIVE ION DRAG AND CURRENT PARTITIONING  
AT THE CATHODE OF A JxB ACCELERATOR

<u>Arc Current I (amp)</u>	<u>Plasma Gas Electrode Material</u>	<u>Gas Pressure (Torr)</u>	<u>Ion Drag at the Cathode (gm)(a)</u>	<u>Ionization Limiting Velocity (cm/sec)</u>	<u>Ion Current Fraction at the Cathode (Percent)</u>
50	Ar - Cu	2	1.67	$8.71 \times 10^5$	9.05
50	He - Cu	8.5	.75	$3.45 \times 10^6$	10.3

(a) Ion Drag = (Cathode Drag - Anode Drag) at  $B \approx 1$  kilogauss

### 3.4 Measurement of Arc Constriction and The Voltage Dependence of Cathode Fall in a Magnetic Field

The electrode damage is related to the geometrical size of the arc at the electrode which in turn depends upon the gas pressure, the arc current and the magnetic field<sup>15</sup>. The analytical study of arc constriction processes is summarized in an earlier part of this report. In this section we summarize the experimental results of these investigations.

The equipment used for the experimental study of arc constriction was available as a result of another research program basically concerned with cathode phenomena in the mercury arc<sup>20</sup>. In return, the analytic results of this program were used to aid in the interpretation of the data obtained from the mercury arc cathode program.

Figure 17 shows the discharge tube located between the pole faces of a 10 kilogauss electromagnet. The cathode consisted of a ground molybdenum anchor in a mercury pool. A flat molybdenum plate was used as the anode. As a result of the cathode geometry it was possible to rotate the cathode spot in the grooved cathode; the current flow in the cathode sheath region was across the magnetic field while the current flow in the plasma column and the anode sheath was parallel to the magnetic field. In this way one could study the effect of magnetic field upon the cathode sheath without using probes; the essential feature of this method is that any variation of arc voltage as a result of magnetic field probably would be predominantly due to the change of cathode fall. It is anticipated that the change of anode fall and of plasma drop would be small because the magnetic field and current flow would be parallel in those regions.

The magnetic field caused the arc to rotate and thus made it possible to study the dimensions of the arc. The rotation was in the retrograde direction.

Prior to mounting the tube on the vacuum system, the electrodes were cleaned electrolytically in a sodium hydroxide solution and were rinsed with clean water. The final treatment of the electrodes consisted of degassing in a

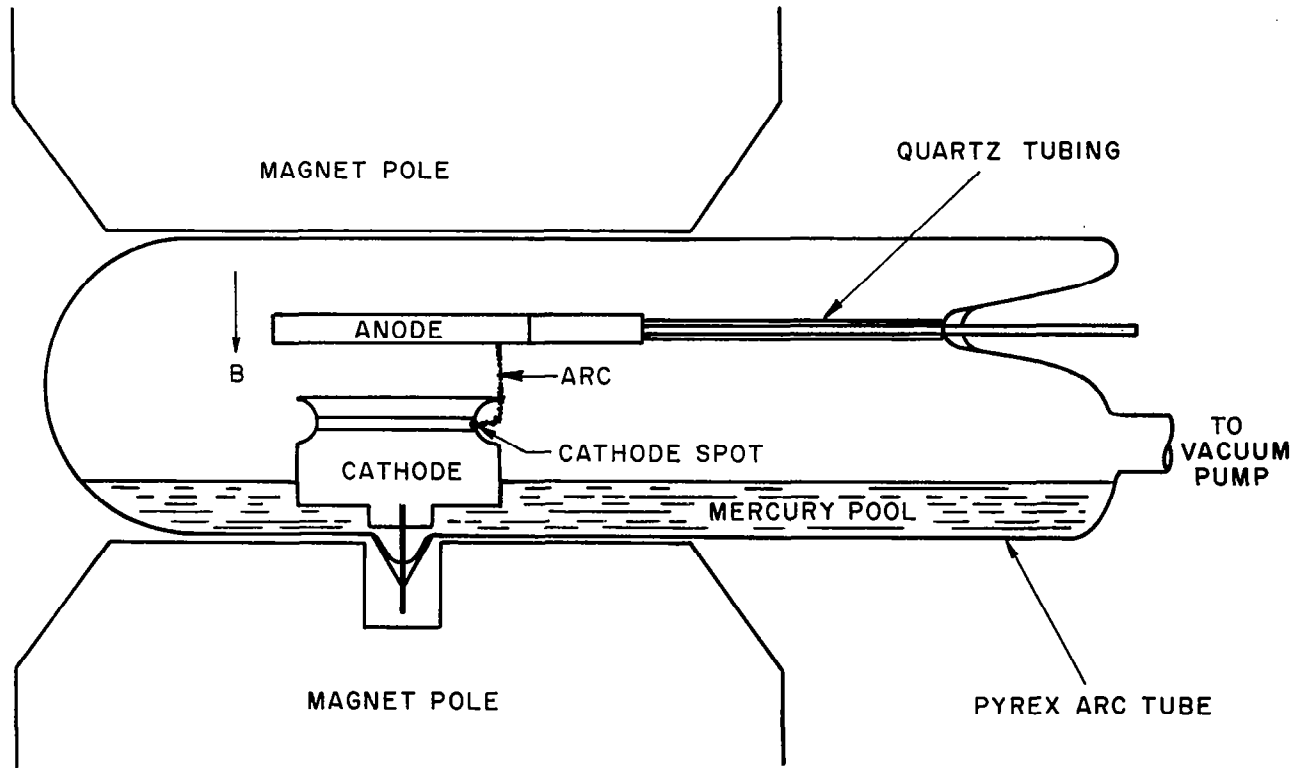


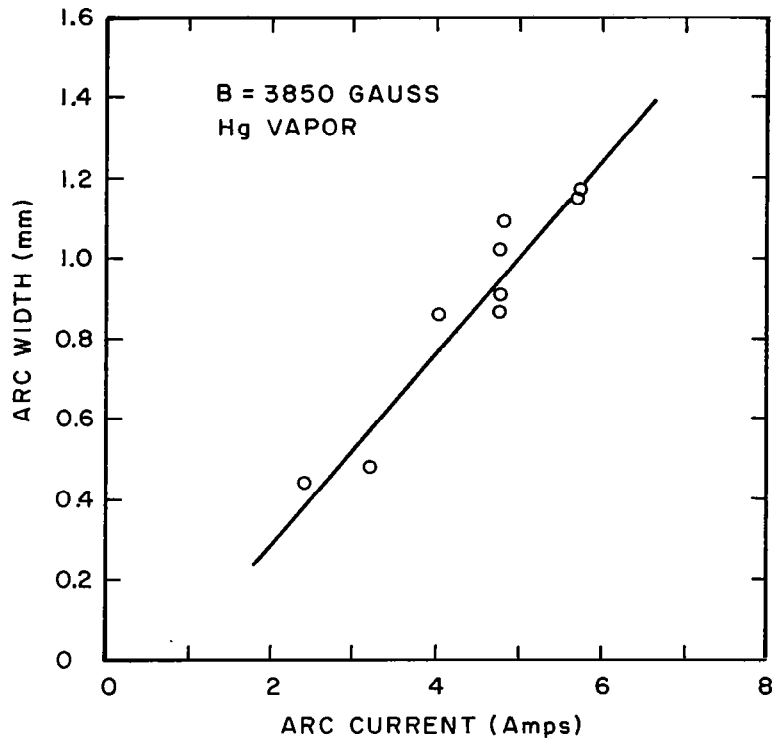
FIGURE 17.  
DRAWING OF A DISCHARGE TUBE SHOWING THE ELECTRODE AND  
MAGNETIC FIELD CONFIGURATION.

continuously pumped system and of arc cleaning with an argon discharge. Mercury was then distilled into the tube to the desired level. This treatment appeared to be satisfactory to the extent that the tube performance was found to be steady and the scatter in the data was reasonably low. Arcs of 2 to 6 amps were studied in mercury vapor plasma in the range 35 to 100 microns.

The dependence of the arc radius was studied as a function of arc current and as a function of magnetic field and of pressure. It was decided to study the arc radius of the plasma near the cathode. Such information was also useful in understanding the emission phenomena at the cathode, which is also of interest in this program. The radius of the luminous core in front of the cathode spot was considered to be the arc radius. Spectral filters were used to look at radiation from the positive ions alone so that the dimensions of the conducting plasma could be measured. The variation in arc radius was measured using 1) integrated photographic and 2) time of flight techniques.

The first method consisted of taking a fast photograph of the arc as it moved around the anchor. The light intensity profile of the luminous band was proportional to the arc radius. The change in width of the light band was interpreted as the change in arc diameter. For the time of flight technique, the arc image was formed on a screen with a small aperture (and a photomultiplier in back). The time taken by the arc to scan across the opening and around the anchor was determined with a CRO and the photomultiplier tube. The width and periodicity of the light signal generated by the moving arc then permitted an evaluation of arc length. The data obtained by these two methods was found to be consistent.

Figure 18 shows the dependence of arc width as a function of arc current at 3850 gauss. Data at high B fields up to 10,000 gauss showed a similar dependence. The data was taken at constant vapor pressure and constant B to study the dependence of arc radius upon arc current alone. The variation of R with I was found to be linear within the accuracy of the experiment and was in agreement with the analytical predictions.



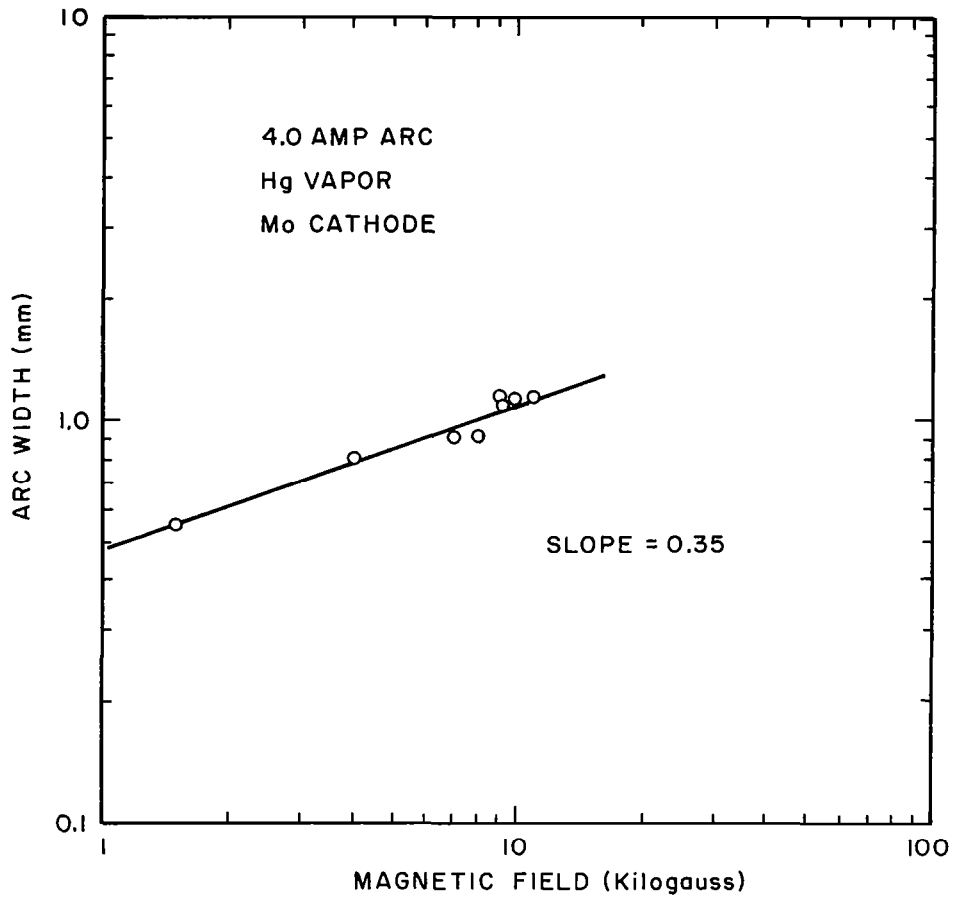
**FIGURE 18.**  
DEPENDENCE OF CATHODE SPOT WIDTH UPON  
ARC CURRENT FOR CONSTANT MAGNETIC  
FIELD AND PRESSURE.

Figure 19 is a plot of  $R$  against the magnetic field at fixed arc current ( $I = 4$  amp) and constant mercury vapor pressure. Again consistent with theory, it is seen that  $R$  increased with  $B$ . The plot is made on a log-log scale and gives an exponent value of about  $1/3$ . In Figure 20 is shown the variation of  $R$  with reduced mercury vapor pressure  $p_0$  for constant  $B$  and  $I$ . The plot shows an inverse power law dependence of  $R$  on  $p_0$ . The exponent has a value of about  $-1/3$ . Thus experimentally it may be concluded that  $R$  varies as a function of  $B/p_0$  in agreement with the analytical theory, and in particular varies as  $(B/p_0)^{1/3}$ .

The dependence of arc voltage on magnetic field for different arc currents and mercury vapor pressure was also studied on the same apparatus. The results of this investigation are presented in Figure 21. Due to the internal heating, the arc voltage was found to depend on the operating time of the tube at each value of magnetic field. This resulted in the non-reproducible data with large scatter. To overcome this difficulty, the voltage was taken in a transient mode so that the slow temperature and pressure rise in the tube did not affect the measurements. Initially the arc was operated at a low standard magnetic field and then switched for a short time to the desired magnetic field. The voltage was quickly read and then the field was returned to the standard magnetic field thus keeping the average tube power essentially constant. By changing the standard magnetic field value, the constant vapor pressure was changed to study the slope  $dV/dB$  for different pressures.

The measurements as shown in Figure 21 indicate that the arc voltage (and therefore presumably the cathode fall) is a linear function of the  $B$  field. This is in agreement with the predictions of the analytical model<sup>26</sup>. The functional dependence of  $dV/dB$  on pressure as  $(p_0)^{-1/2}$  also appears to be in agreement with the physical model considered in this study.

The wear and damage to the arc electrode is related to the constricted nature of the anode spot and cathode spot. It has been shown that the constriction of the arc can be predicted on the basis of conservation of energy .



**FIGURE 19.**  
DEPENDENCE OF ARC WIDTH UPON MAGNETIC  
FIELD FOR CONSTANT PRESSURE AND ARC CURRENT.

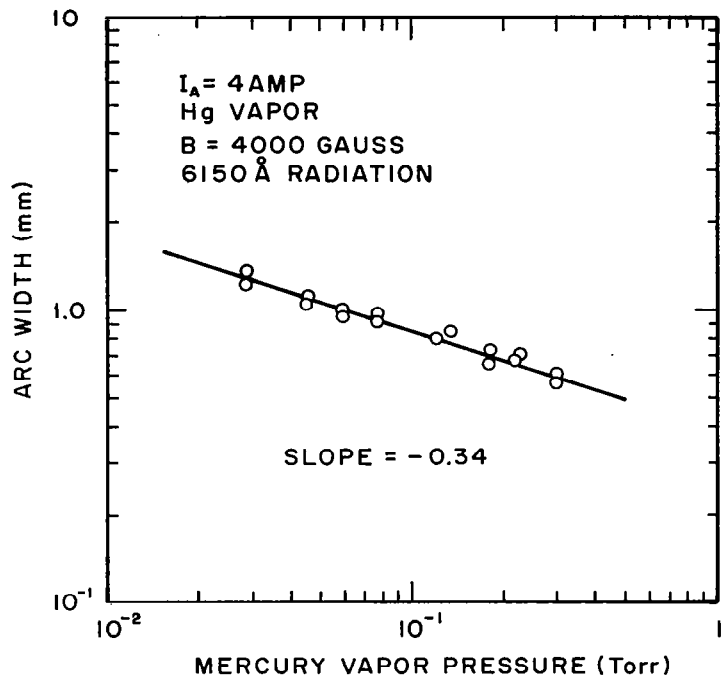


FIGURE 20.  
 VARIATION OF ARC WIDTH AS A FUNCTION OF  
 MERCURY VAPOR PRESSURE (FOR CONSTANT  
 MAGNETIC FIELD AND ARC CURRENT).

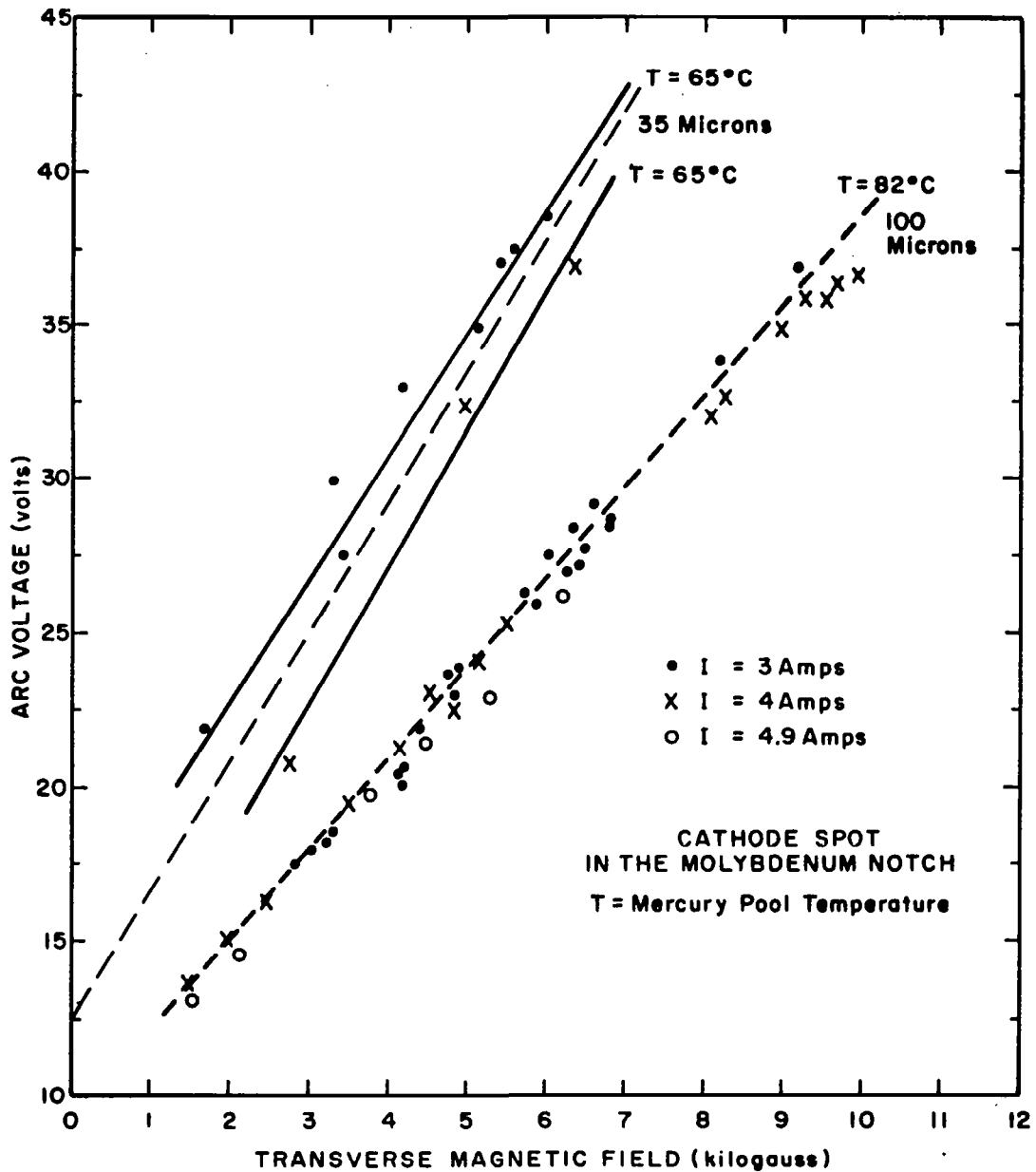


FIGURE 21.  
 DEPENDENCE OF ARC VOLTAGE UPON TRANSVERSE  
 MAGNETIC FIELD AND UPON MERCURY  
 VAPOR PRESSURE.

The energy density transferred to the cathode spot is also related to the cathode fall. This cathode fall appears to be significantly increased by a transverse magnetic field, particularly at the lower pressure.

#### 4. SUMMARY

The interactions of moving plasmas with physical boundaries have been studied both theoretically and experimentally. The positive ions have been shown to play an important role in various plasma boundary interactions.

The criteria for the formation of a general sheath are determined by the positive ion current flow as well as by the reflection and emission coefficients of the particles at the surface.

A new and more general criterion for the plasma sheath has been established, which contains the well known "Bohm's Sheath Criterion" as a special limit. In order to be able to retain ionization effects in a microscopic analysis, a new set of kinetic equations for ions, electrons, and neutral particles was constructed. These equations should prove valuable in the future analysis of the sheath and the near sheath, where ionization effects play an important role.

The tangential drag due to positive ions at the cathode was directly measured and was shown to be an appreciable fraction of the total drag force on the plasma. The anode drag was also measured as a function of various arc parameters and it was shown that the total cathode drag force is larger than the anode drag force. With the aid of assumptions about the transverse arc velocity and the momentum accommodation coefficient, it was possible to deduce the ion current partitioning at the cathode and to show that the ion current is about 10% of the total current.

A special design was devised for the electrode insulators in order to extend the operating life time. An analysis was made of the various modes of energy transport to the electrode and it was concluded that in typical arc cases, the electrons and the ions played dominant roles.

The various mechanisms of electron emission at the cathode spot were studied and it was concluded that thermionic or field emission alone could not be used as an explanation. It was concluded that the positive ion current played a dominant role in the various electron emission processes. A model involving ion-

micro field emission was developed and was shown to be capable of explaining the electron emission. It is recommended that this model be further investigated.

The role of arc retrograde motion was briefly studied to determine its possible effect on the tangential electrode forces. It was concluded that phenomena of the arc retrograde motion in a magnetic field can be explained in terms of a plasma phase propagation in the direction of larger magnetic fields where the ambipolar diffusion loss is smaller.

The problem of arc constriction at the electrode was considered in order to study the causes of the constriction and of the resulting large energy flux density. It was possible to predict the dependence of the constriction upon the arc current, the E field, and the magnetic field over various operating ranges. It was shown that the constriction can be explained in terms of a balance between the ohmic energy input and the various modes of energy loss. Experimental data was used to test the predicted dependence of arc diameter upon arc current and upon transverse magnetic field. The effect of a transverse magnetic field upon the cathode fall was briefly studied theoretically and experimentally and it was shown that the transverse magnetic field increased the cathode fall.

## ACKNOWLEDGMENT

This research was supported by the National Aeronautics and Space Administration under Contract NASw-1014 to Space Sciences, Inc. (1964 - 1966). It is our pleasure to express our gratitude to the National Aeronautics and Space Administration for their financial support, and to Professor H. Grad of the Courant Institute of New York University for his many valuable suggestions and constructive comments throughout the program. In addition, we are happy to acknowledge the suggestions of Dr. K. Thom and his coworkers of the National Aeronautics and Space Administration leading to the basic concept for the electrode drag measurement experiment. The skillful assistance of Mr. James Dodge and of Miss Ellen Parent has been of considerable value.

## REFERENCES

1. Hu, P. N. and Ziering, S., "Collisionless Theory of a Plasma Sheath Near an Electrode", *Phys. of Fluids*, 9, 2168 (1966).
2. Hu, P. N. and Ziering, S., "The Plasma Sheath for Transverse Flows," Annual Meeting of the Div. of Plasma Physics of the A.P.S. (Boston, Nov. 1966).
3. Hu, P. N. and Ziering, S., "Kinetic Model for Three-Component Plasmas with Ionization," *Phys. of Fluids*, 9, 1983 (1966).
4. Thom, K. Norwood, J. and Jalufka, N., *Phys. of Fluids*, Supplement S67, (1964).
5. Rohatgi, V. and Aisenberg, S., "Composite Metallic and Dielectric Insulators for High Current Arc Electrodes," *Rev. Sci. Instr.*, 37, 1603 (1966).
6. Spitzer, L., Jr., Physics of Fully Ionized Gases (Inter-Science, New York, 1956).
7. Kisliuk, P., *J. Appl. Phys.*, 30, 51 (1959).
8. Ecker G., "Electrode Components of the Arc Discharge", in *Ergenbnisse der Exakten Naturwissenschaften*, Vol.33, (Springer, Berlin, 1961).
9. Mackeown, S. S., *Phys. Rev.*, 34, (1929) p. 611.
10. Brown, S. C., Basic Data of Plasma Physics, (M.I.T. Press, 1959) p. 315.
11. Weissman, I., *J. App. Phys.*, 36, 406 (1965).
12. Honig, R. E., *RCA Review*, 23, (1962) p. 574.
13. Ecker G. and Muller, K. G. , *J. Appl. Phys.*, 30, 1466 (1959).
14. Good, R. H. and Muller, E. W., Field Emission, in *Handbuch der Physik*, Vol. 21, (Springer, Berlin, 1956).
15. Aisenberg, S. and Rohatgi, V., "A Study of Arc Constriction Processes," *Seventh Symposium on Engineering Aspects of Magnetohydrodynamics*, Princeton, New Jersey (1966).
16. Finkelburg, W. and Mæecker, H., "Electric Arcs and Thermal Plasmas," *Handbuch der physik*, Vol. 22, (Springer-Ver Lag, 1956).

17. Finkelnburg, W. and Maecker, H., "Electric Arcs and Thermal Plasma," Translated by B. H. Eckstein, Aeronautical Research Lab., Office of Aerospace Research, ARL 62-302(1962).
18. Spenke, E., Z. Physik, 127, (1950) p. 221.
19. Allis, W. P., "Motions of Ions and Electrons" Handbuch der Physik, Vol. 21, (Springer, Berlin, 1956).
20. Afshartous, Aisenberg, Rohatgi, and Smith, "Investigation of Cathode Phenomenon in the Mercury Arc," Contract No. AF30(602)-3093.
21. Froome, K. D., Proc. Phy. Soc., 62, 805 (1949).
22. Milliaris, A. C., ARL Technical Report 64-216 (1964).
23. Kennard, E. H., Kinetic Theory of Gases, (McGraw-Hill, N.Y., 1938). p. 311.
24. Stark, J., Physik, Z., 4, 440 (1903).
25. Sommerville, J. M., The Electric Arc, (Methuen and Co., Ltd., London, 1959) p. 82.
26. Aisenberg, S. Hu, P., Rohatgi, V. and Ziering, S., "A Study of Electrode Effects in Crossed Field Accelerators Summary Report," SSI-152-SR, September 1965.
27. Aisenberg, S. and Rohatgi, V., "Measured Tangential Electrode Forces for an Arc in a Transverse Magnetic Field," Appl. Phys. Letters, 194, (1966).
28. Rosebury, Fred, "Handbook of Electron Tube and Vacuum Techniques" (Addison-Wesley Publishing Co., Inc. 1965) p. 195.
29. Lin, S. C., "Limiting Velocity for a Rotating Plasma," Phy. Fluids, 4, 1277 (1961).
30. Lehnert, B., "Ionization Process of a Plasma," Phy. Fluids, 9, 774 (1966).

31. Sutton, G. W. and Sherman, A., Engineering Magnetohydrodynamics, (McGraw-Hill, New York, 1965) p. 95.
32. Boule, Ann Physik, 44, 145 (1914)
33. Lee, T. H., "T-F Theory of Electron Emission in High Current Arcs," Journal App. Phy., 30, 1966 (1959).

*"The aeronautical and space activities of the United States shall be conducted so as to contribute . . . to the expansion of human knowledge of phenomena in the atmosphere and space. The Administration shall provide for the widest practicable and appropriate dissemination of information concerning its activities and the results thereof."*

—NATIONAL AERONAUTICS AND SPACE ACT OF 1958

## NASA SCIENTIFIC AND TECHNICAL PUBLICATIONS

**TECHNICAL REPORTS:** Scientific and technical information considered important, complete, and a lasting contribution to existing knowledge.

**TECHNICAL NOTES:** Information less broad in scope but nevertheless of importance as a contribution to existing knowledge.

**TECHNICAL MEMORANDUMS:** Information receiving limited distribution because of preliminary data, security classification, or other reasons.

**CONTRACTOR REPORTS:** Scientific and technical information generated under a NASA contract or grant and considered an important contribution to existing knowledge.

**TECHNICAL TRANSLATIONS:** Information published in a foreign language considered to merit NASA distribution in English.

**SPECIAL PUBLICATIONS:** Information derived from or of value to NASA activities. Publications include conference proceedings, monographs, data compilations, handbooks, sourcebooks, and special bibliographies.

**TECHNOLOGY UTILIZATION PUBLICATIONS:** Information on technology used by NASA that may be of particular interest in commercial and other non-aerospace applications. Publications include Tech Briefs, Technology Utilization Reports and Notes, and Technology Surveys.

*Details on the availability of these publications may be obtained from:*

SCIENTIFIC AND TECHNICAL INFORMATION DIVISION  
NATIONAL AERONAUTICS AND SPACE ADMINISTRATION  
Washington, D.C. 20546